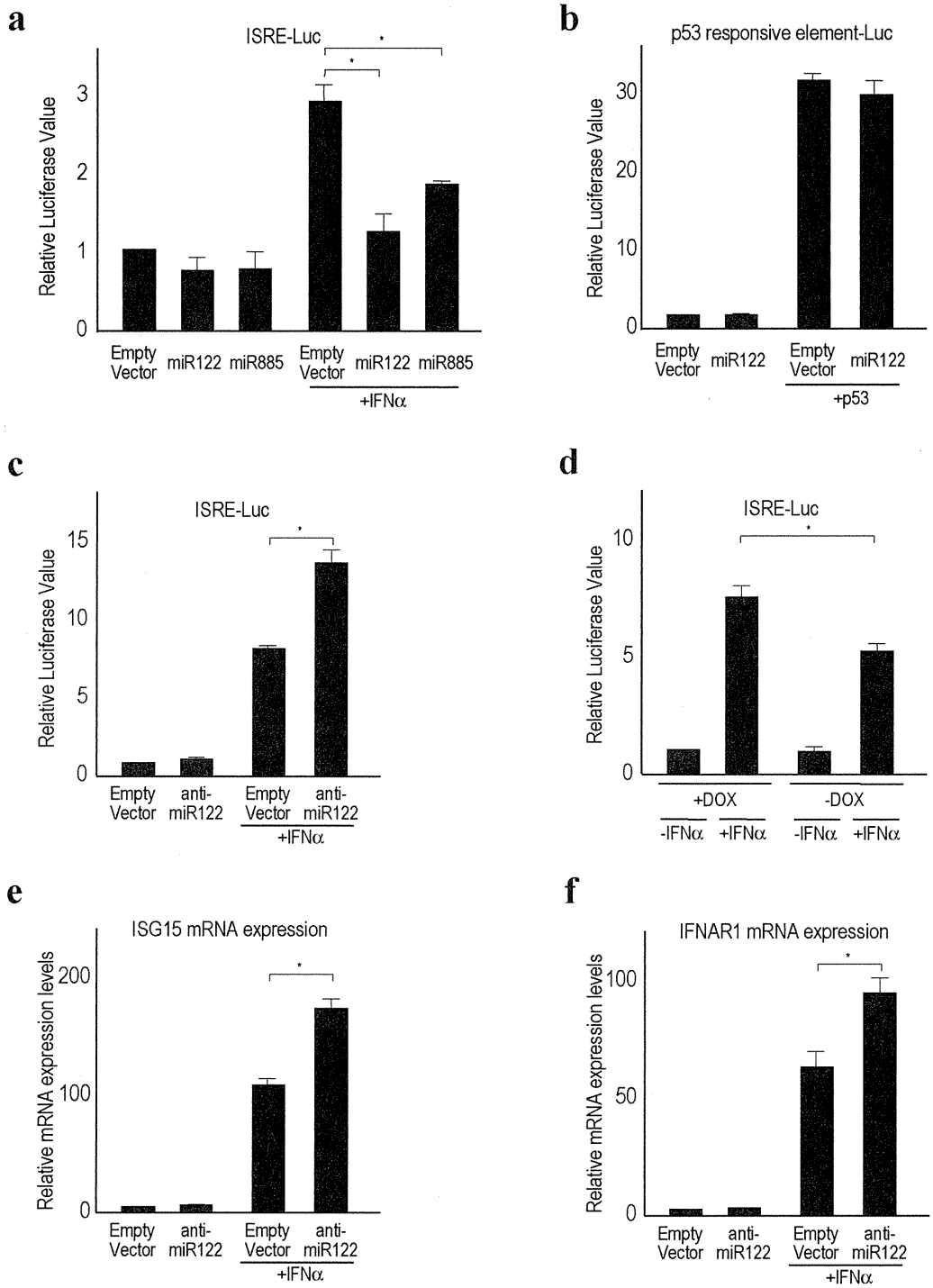

Figure 2 | MiR122 modulates ISRE activities. (a) Overexpression of the selected microRNA precursors suppresses ISRE activity following IFN-α stimulation. ISRE reporter plasmids were transiently transfected, with or without selected microRNA precursor-expressing plasmids, into Huh7 cells. Luciferase values were normalized to those of cells transfected with an empty vector and without IFN, which were set to 1. *, $p < 0.05$. Data represent the means ± standard deviations (SD) of three independent determinations. Similar results were obtained using HepG2 cells. (b) p53 activities were unaffected by miR122 expression. Reporter assays were performed with p53 reporter and p53 expressing plasmids with or without miR122 precursor expression in Huh7 cells. Data represent the means ± SD of three independent determinations. (c) Silencing of miR122 function enhances ISRE activity. Anti-miR122 expressing plasmids were used to perform an ISRE reporter assay in Huh7 cells. *, $p < 0.05$. Data represent the means ± SD of three independent determinations. (d) Hela-Tet-Off-miR122 precursor cell lines were used to measure ISRE activity. Cells were transfected with ISRE reporter constructs with (DOX+) or without (DOX-) doxycyclin. DOX+ shut off the miR122 expression in these cells. The reporter activities after 6 h of IFN-α stimulation were compared. *, $p < 0.05$. Data represent the means ± SD of three independent determinations. (e, f) IFN-inducible genes (e, ISG15; f, IFNAR1) were more induced in miR122-silenced Huh7 cells, determined by quantitative RT-PCR using RNA after 6 h of IFN-α stimulation. *, $p < 0.05$. Data represent the means ± SD of three independent determinations.

Table 1 | Top 30 genes with promoters differentially methylated in control and miR122-silenced Huh7 cells. Values indicate methylation levels. Values in 'Differences' indicate quantitative differences in methylation levels of target gene CpG sites. Higher values indicate greater methylation levels. Genes in bold and highlighted in gray means greater methylation; others were less methylated in miR122-silenced Huh7 cells

SYMBOL	Control	miR122-silenced	Difference	CpG ISLAND LOCATIONS
GPC3	0.4242135	0.11596	0.3082535	X:132946499-132947763
FLJ30058	0.4155016	0.1428133	0.2726883	X:130019792-130020537
EIF3S6IP	0.672594	0.4012034	0.2713906	22:36574299-36576077
BHLHB9	0.3481071	0.07687688	0.27123022	X:101862184-101862707
PORCN	0.6389685	0.3697215	0.269247	
MSI2	0.4593301	0.1955636	0.2637665	17:52688030-52689554
DNTT	0.6114385	0.3489618	0.2624767	10:98054238-98054478
SEMA3B	0.3901392	0.1301293	0.2600099	3:50285369-50286362
RYR2	0.4331115	0.1756537	0.2574578	1:235271651-235273428
TCEAL7	0.6519198	0.4006093	0.2513105	
NR0B2	0.3711949	0.1234481	0.2477468	
SOCS3	**0.1831344**	**0.4273662**	**0.2442318**	17:73866027-73868731
TAS2R16	0.5821649	0.3380581	0.2441068	
BHLHB9	0.3021148	0.06171004	0.24040476	X:101862184-101862707
OR12D3	0.5266486	0.2884241	0.2382245	
ADAMTSL1	0.4537211	0.2196532	0.2340679	
TBX6	0.5031447	0.2695281	0.2336166	16:30010427-30011656
ICAM4	0.4990334	0.2668367	0.2321967	19:10258558-10259935
C9orf125	**0.2387415**	**0.4707038**	**0.2319623**	9:103287963-103289481
ELN	**0.1332373**	**0.3629701**	**0.2297328**	7:73080116-73080605
ANKRD30A	0.898423	0.6711555	0.2272675	10:37453955-37454965
OR10J1	0.5324367	0.3094136	0.2230231	
TP73	0.3596564	0.1386476	0.2210088	1:3596889-3597535
CNNM1	0.6313883	0.4106784	0.2207099	10:101078809-101080801
DHH	0.2955738	0.07619943	0.21937437	12:47774151-47774653
CTAG2	0.5303309	0.3110451	0.2192858	X:153536438-153536702
GNB4	0.3091451	0.09039365	0.21875145	3:180651316-180652496
PNPLA2	0.4458646	0.2272328	0.2186318	11:808884-809164
FGF7	0.6298472	0.4128944	0.2169528	
NTE	0.4557684	0.2400911	0.2156773	19:7504300-7507429

significantly increased methylation levels were observed in the promoter of the SOCS3 gene, which is a negative regulator of IFN signaling. The enhanced methylation levels in silencing miR122 were confirmed by bisulphite sequencing at the CpG island in the SOCS3 promoter, from −556 to −335 relative to the transcriptional start site (Fig. 3a and b). Thus, we hypothesized that the greater methylation of SOCS3 induced by miR122 silencing results in decreased expression of SOCS3 protein, which may, in turn, enhance IFN-α signaling.

MiR122 silencing enhances STAT3 activation by decreasing SOCS3 expression. To confirm the above results, we examined SOCS3 expression and IFN signaling-related molecules in miR122-silenced Huh7 cells (Fig 4a). While the GEO database contained no direct data regarding SOCS3 cDNA expression, we found decreased SOCS3 protein levels in miR122-silenced cells, consistent with promoter hyper-methylation (Fig. 4a). Although the mechanisms underlying the altered methylation induced by miR122 silencing remain unknown, it did not depend on DNA methyltransferase 1 (Dnmt1), which is a key mediator of DNA methylation that catalyzes the methylation of CpG dinucleotides in genomic DNA[27], because the decreased SOCS3 expression by miR122 silencing was also present in Dnmt1 knockdown cells (Fig. 4b).

Because SOCS3 is a potent inhibitor of STAT3 activation[6], and because type I IFNs induce STAT3 as well as STAT1 and STAT2 activation[5,28], we examined the phosphorylation status of STAT proteins after IFN treatment in Huh7 control and miR122-silenced cells (Fig. 4a). While the STAT1, 2, and 3 protein levels and the phosphorylation levels of STAT1 before and after IFN-α stimulation in these two cell lines did not differ significantly, STAT3 phosphorylation levels were higher in miR122-silenced cells 1 and 6 h after IFN-α stimulation, consistent with the decreased expression of SOCS3 (Fig. 4a). Furthermore, STAT2 phosphorylation was slightly higher in miR122-silenced cells (Fig. 4a). Similar tendencies were also observed after treatment with IFN-β, another type I IFN. These data suggest that IFN-α treatment induced greater STAT3 activation in miR122-silenced cells, probably due to decreased SOCS3 expression.

In contrast, whereas IFN-γ (type II IFN) and IFN-λ (type III IFN) induced slight phosphorylation of STAT1 and STAT3, the levels in control and miR122-silenced cells were comparable. STAT2 protein levels were significantly lower in miR122-silenced cells than in controls after treatment with these cytokines (Fig. 4a). No induction of SOCS3 after treatment with IFN-α/β, IFN-γ, or IFN-λ was detected in miR122-silenced cells, probably due to promoter methylation (Fig. 4a), whereas SOCS3 protein was induced by all IFNs in control cells (Fig. 4a). Because increased expression of miR122 was detected after IFN-λ stimulation (Fig. 4c), this might be responsible for the increased SOCS3 expression induced by IFN-λ stimulation.

To confirm whether the induction of the enhanced ISRE activity in miR122-silencing was dependent on the decreased expression of SOCS3, we investigated whether the restoration of SOCS3 expression in miR122-silencing could reduce the ISRE activity in a reporter assay. The overexpression of SOCS3 in miR122-silenced Huh7 cells reduced the induction of ISRE activity caused by miR122-silencing (Fig. 5a and b), although we could not fully exclude the possibility that other mechanisms were also involved because the reversal of ISRE activity did not completely reach the level of the control. To support this, we confirmed the restoration of STAT2 and STAT3 phosphorylation levels induced by IFN-α treatment in miR122-silenced cells that stably overexpressed SOCS3 (Fig. 5c). These results suggest that the enhanced ISRE activity in miR122-silenced cells is

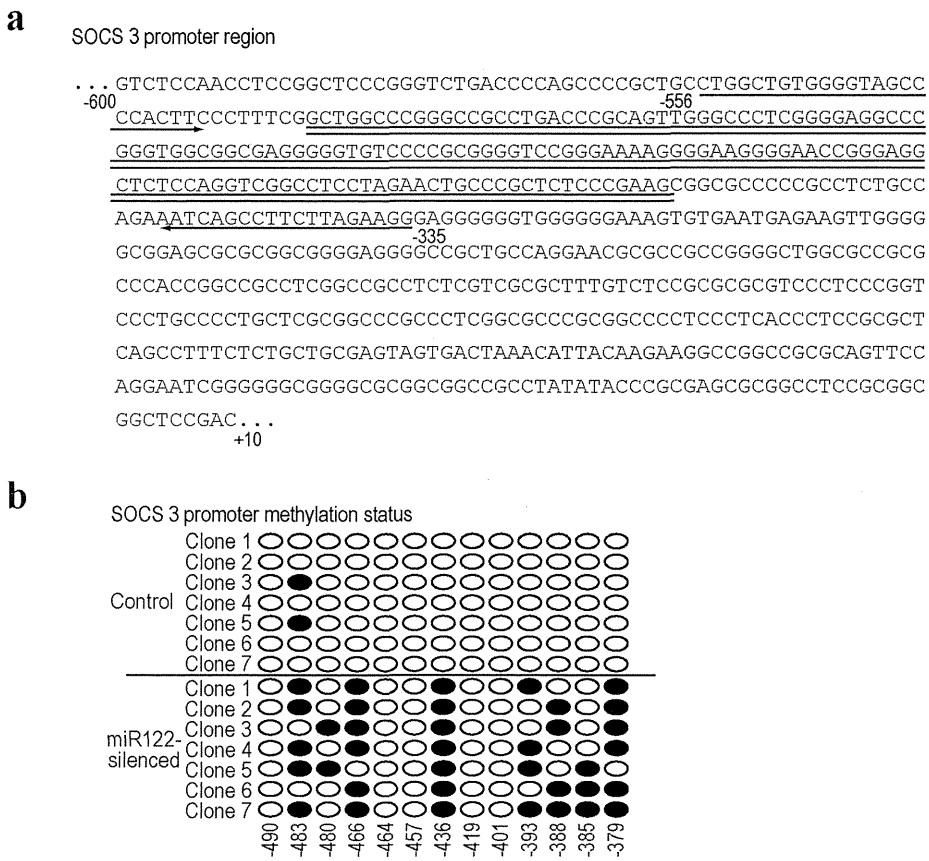

Figure 3 | CpG methylation status in the SOCS3 promoter. (a) The CpG island in the SOCS3 promoter is indicated by double underlines. The numbers are the positions relative to the transcription start site. Primers used for the bisulphate sequences in this study are indicated by arrows. (b) Methylation status in the CpG island of the SOCS3 promoter in control and miR122-silenced Huh7 cells, determined by the bisulphate sequences. Seven clones each were sequenced. Circles represent CpG sites. Black circles, methylated CpG sites.

mostly, if not completely, dependent on the reduced expression of SOCS3.

MiR122 silencing enhances ISGF3-DNA binding. Type I IFNs (IFN-α and -β) activate STATs by phosphorylation, followed by formation of the ISGF3 complex, which is composed of STAT1, STAT2, and IRF9. The importance of ISGF3 in antiviral responses is well established[29]. In contrast, the precise role of STAT3 in type I IFN signaling is not completely understood[30]. However, numerous clinicopathological results suggest that increased SOCS3 expression in the liver is closely related to a poor response to IFN therapy for HCV eradication[8,9]. This in turn suggests that high SOCS3 expression and low STAT3 activation may be related to impaired ISGF3 complex activation. In addition, STAT3 activation supports the ISGF3-dependent induction of antiviral genes *in vitro*[31]. Based on these reports, and because SOCS3 expression was lower in miR122-silenced cells (Fig. 4), we hypothesized that the level of ISGF3 complex after IFN-α treatment is higher in miR122-silenced cells, leading to greater ISRE activation (Fig. 2). While the levels of Oct-1-DNA binding as a loading control were not changed, activation of ISGF3 binding to an ISRE-containing oligonucleotide after IFN-α treatment was significantly greater in miR122-silenced cells (Fig. 6a, b, c), consistent with the fact that ISRE activities were enhanced in miR122-silenced cells in a reporter assay (Fig. 2). These data suggest that miR122-silencing in hepatocytes results in low SOCS3 expression via promoter methylation, which may subsequently enhance the induction of IFN-stimulated gene expression by increasing ISGF3-ISRE binding activities triggered by type I IFN treatment.

Discussion

Although the treatment options for HCV infection are changing due to the introduction of HCV protease inhibitors and DAAs, the principal drug for HCV therapy remains IFN. In this study, we demonstrated that the reduced expression of miR122 contributes to decreased SOCS3 expression via promoter methylation and, subsequently, enhanced ISRE activity results after IFN-α stimulation. These data provide a molecular rationale for, and a method for increasing the efficacy of, IFN therapy for HCV infection.

MicroRNAs are involved in various biologically important intracellular signaling pathways[15–18]. Regarding the convergence of microRNAs and IFN signaling, some microRNAs are reported to be involved in endogenous IFN production in the innate immune response induced by pathogen infection[32]. In addition, several microRNAs that may regulate genes that have anti-pathogen effects are induced by IFN stimulation[33]. In this study, however, the level of miR122 expression seemed to determine the efficacy of the signaling triggered by the exogenous IFN used as an anti-HCV therapy.

MiR122 is the most abundant microRNA in the liver[24], where it has many important biological roles, such as in fatty acid metabolism[26,34] and circadian rhythms[35] under normal conditions. Further, it is also a determinant of the biological aggressiveness of hepatocellular carcinoma[36] in the pathological state. In general, microRNAs act as repressors of target gene expression[37]. However, regarding miR122 and HCV, miR122 somehow enhanced HCV RNA replication in an *in vitro* replicon system[38]. Although the precise molecular mechanisms underlying this phenomenon remain unknown, antisense miR122 has been developed as a therapeutic drug for HCV based

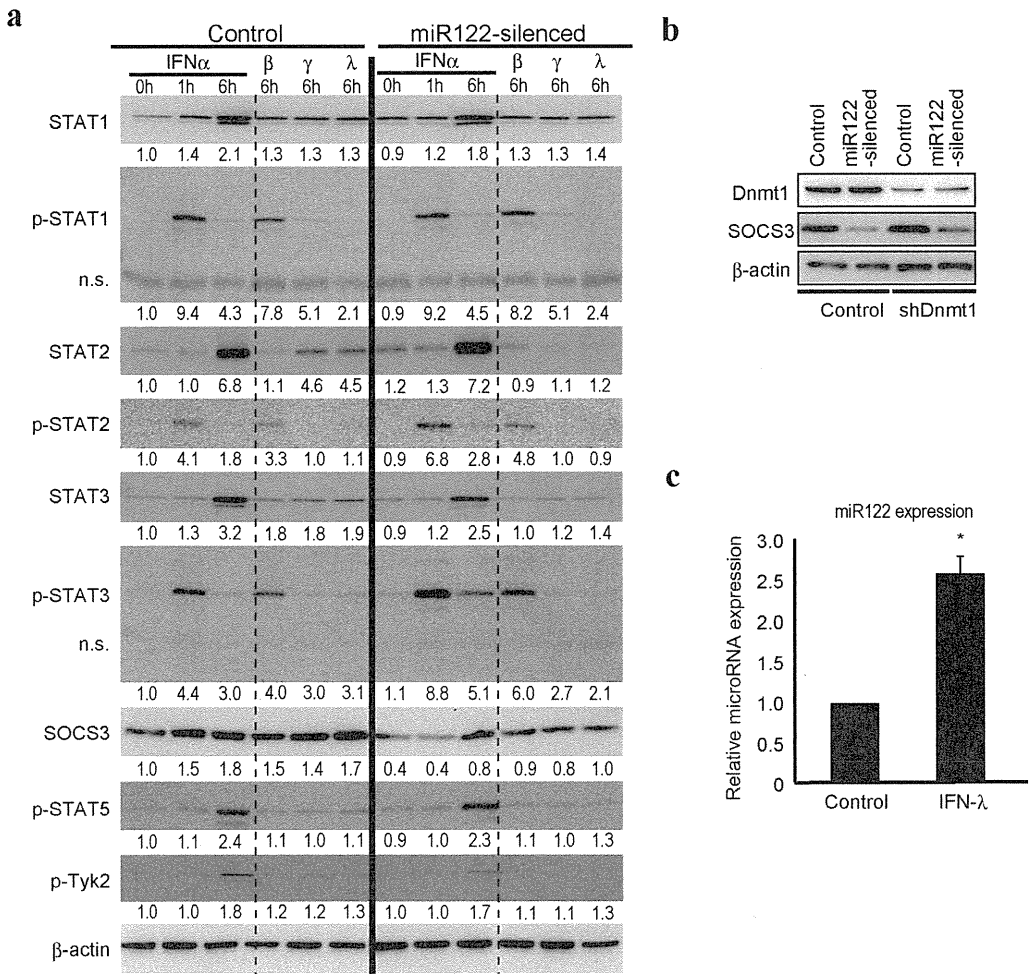

Figure 4 | SOCS3 expression is decreased by miR122 silencing. (a) Protein levels of the indicated IFN signaling-related genes were determined using control and miR122-silenced Huh7 cells after IFN-α, β, γ, or λ stimulation at the indicated time points. A representative of three independent determinations is shown. n.s. indicates non-specific bands. The band intensities were quantitated and adjusted by the expression levels of β-actin. The calculated ratios are indicated below each panel after setting the value of control cells at 0 h as 1.0. (b) Dnmt1 was not involved in the SOCS3 promoter methylation induced by miR122 silencing. SOCS3 protein levels were determined using control, miR122-silenced, Dnmt1 knocked-down, and Dnmt1 knocked-down with miR122-silenced Huh7 cell lysates. A representative of three independent determinations is shown. (c) MiR122 expression levels after IFN-λ stimulation for 6 h in Huh7 cells were determined by quantitative RT-PCR. Results were calculated by normalizing to U6 amounts and the relative ratio was determined by setting the value of unstimulated cells as 1. Data represent the mean ± SD of three independent determinations. *, $p < 0.05$.

on *in vitro* data[39]. Indeed, treatment of chronically HCV-infected chimpanzees with a locked nucleic acid (LNA)-modified oligonucleotide (SPC3649) complementary to miR122 leads to long-lasting suppression of HCV viremia[39]. Development of this drug for human use is now in Phase IIa trials[40]. Because our results showed that lower expression of miR122 leads to augmentation of the intracellular signaling induced by IFN, a combination therapy consisting of an antisense of miR122 and type I IFNs represents a promising and realistic therapeutic option. In addition, because IFN-α/β was reported to suppress miR122 expression, which is considered one of the mechanisms of action of IFN against HCV[41], the effects of exogenous IFN may be self-augmented by the decreased expression of SOCS3 due to decreased miR122 expression. High expression levels of SOCS3 in the liver are negative predictors of IFN treatment of HCV infection[8,9]. This may reflect suppression of IFN signaling by the high miR122 levels in the liver, as suggested by our data.

Our results indicate that reduced miR122 function leads to promoter methylation and decreased SOCS3 expression, which is possibly not the direct target of miR122, because no predictable sites for miR122 interaction in its 3′UTR were found in a computational search. A hypothesis involving an epigenetics-microRNA regulatory circuit has emerged recently[20]. While a number of microRNAs are regulated epigenetically, others simultaneously regulate epigenetic pathway-related molecules. Taken together, these results suggest that post-transcriptional regulation by microRNAs and transcriptional control machinery by epigenetics cooperate to determine the global gene expression profile and to maintain physiological functions in cells[20]. In our genome-wide study, methylation levels of a subset of gene CpG islands were aberrantly induced by miR122 silencing. While our data suggest that SOCS3 methylation was not mediated by Dnmt1, the precise mechanisms of the aberrant methylation induced by miR122, including whether it operates through regulation of the expression of other genes or directly in the nucleus, remains to be elucidated. Nonetheless, our results indicate that aberrant functions of some miRNAs may lead to changes in the methylation levels of a subset of gene CpG islands.

Recent genome-wide association studies have discovered a significant association between the response to pegIFN and ribavirin

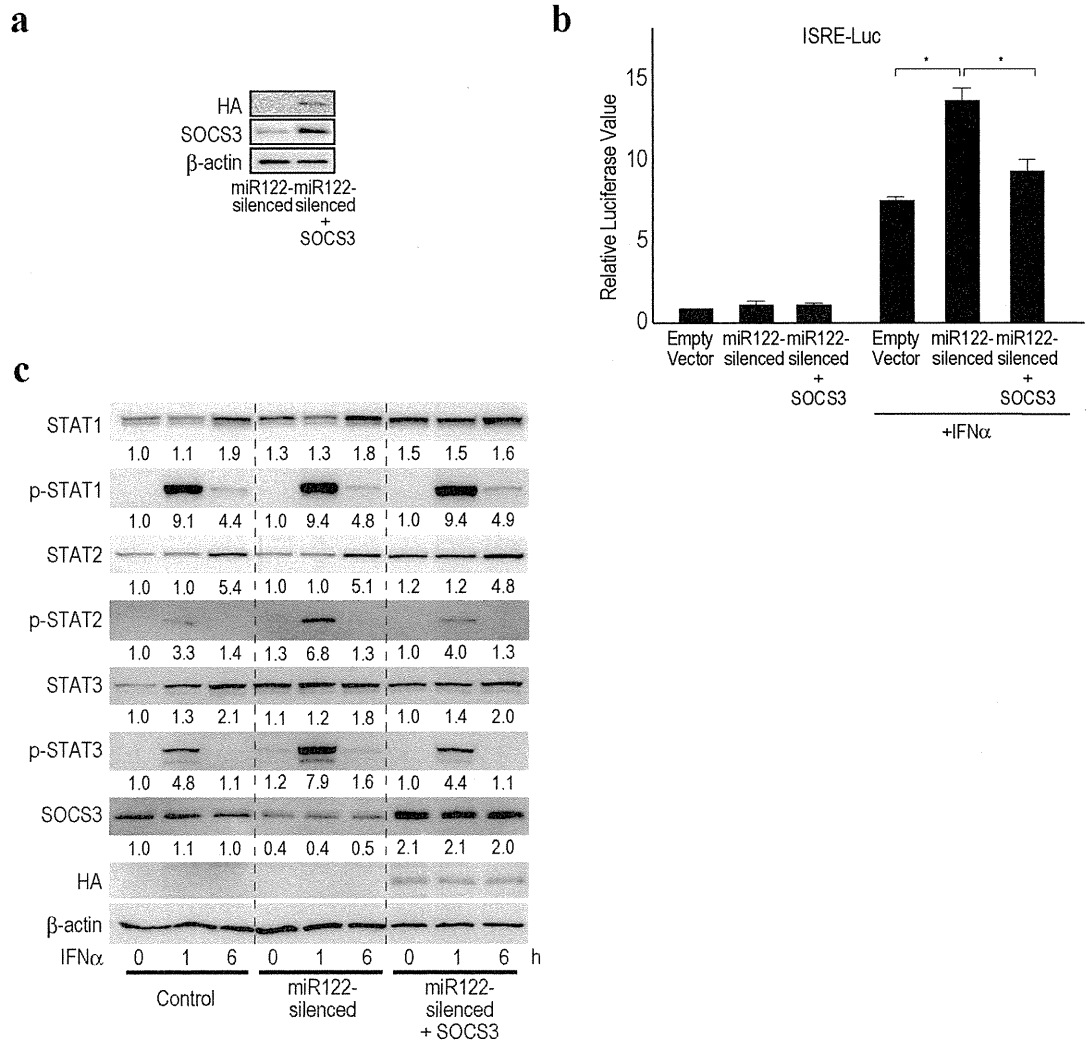

Figure 5 | SOCS3 overexpression in miR122-silenced Huh7 cells reverses enhanced ISRE activities. (a) HA-tagged SOCS3 was overexpressed in miR122-silenced Huh7 cells. Representative blotting images are shown. (b) SOCS3 overexpression suppresses enhanced ISRE activities in miR122-silenced Huh7 cells by a reporter assay. *, $p < 0.05$. Data represent the means ± SD of three independent determinations. (c) SOCS3 overexpression restored STAT2 and STAT3 phosphorylation levels induced by IFN-α in miR122-sileced Huh7 cells. A representative of three independent determinations is shown. The band intensities were quantitated and adjusted by the expression levels of β-actin. The calculated ratios are indicated below each panel after setting the value of control cells at 0 h as 1.0.

therapy and common single nucleotide polymorphisms in the vicinity of IL-28 (IFN-λ) genes[42,43]. In addition, carriers of the alleles associated with resolution of HCV infection have increased serum IFN-λ levels[43]. Our results demonstrate that IFN-λ stimulation increases SOCS3 and miR122 expression, which may block innate type I IFN signaling. This seems inconsistent with the fact that patients with high IFN-λ levels have better responses to pegIFN and ribavirin therapy. However, we speculate that blockade of innate IFN-α signaling by high IFN-λ through SOCS3 expression may prevent the chronically low levels of innate IFN-α, which may increase the sensitivity to exogenous IFN-α when applied in therapeutic quantities. Although further work is required, it is consistent with the fact that low expression of hepatic IFN-stimulated genes (ISGs) is strongly associated with a better response to IFN treatment and genetic variation in IL-28B[44,45].

Higher expression of α-fetoprotein (AFP) is also known as a poor prognostic factor for IFN treatment in HCV therapy[46,47]. As we described previously, decreased expression levels of miR122 are linked to increased expression of AFP[36]. Therefore, in cases with higher AFP levels, miR122 levels in hepatocytes may be low and thus, innate IFN signaling may be high through SOCS3 promoter methylation. These may provide a molecular explanation of the poor response to IFN therapy in cases with high AFP levels.

In summary, our study provides information on the involvement of miR122 in the regulation of ISRE activity through the modulation of SOCS3 expression via gene promoter methylation. Our results provide a molecular rationale that will facilitate more effective use of IFN as an anti-HCV combination therapy, specifically by including modulators of miR122 function.

Methods

Cell culture. The human hepatocellular carcinoma cell lines Huh7 and HepG2 were obtained from the Japanese Collection of Research Bioresources (JCRB, Osaka, Japan). The human embryonic kidney cell line 293T was obtained from the American Type Culture Collection (ATCC, Rockville, MD). MiR122 functionally knocked-down Huh7 (miR122-silenced Huh7) cell lines were as described previously[36]. Hela-Tet-Off cell lines were purchased from Clontech (Mountain View, CA). Huh7-Tet-Off cell lines were established by transfecting with the pTet-Off vector (Clontech) and selecting with 400 μg/ml G418 (Wako, Osaka, Japan). All cells were maintained in Dulbecco's modified Eagle's medium, supplemented with 10% fetal bovine serum.

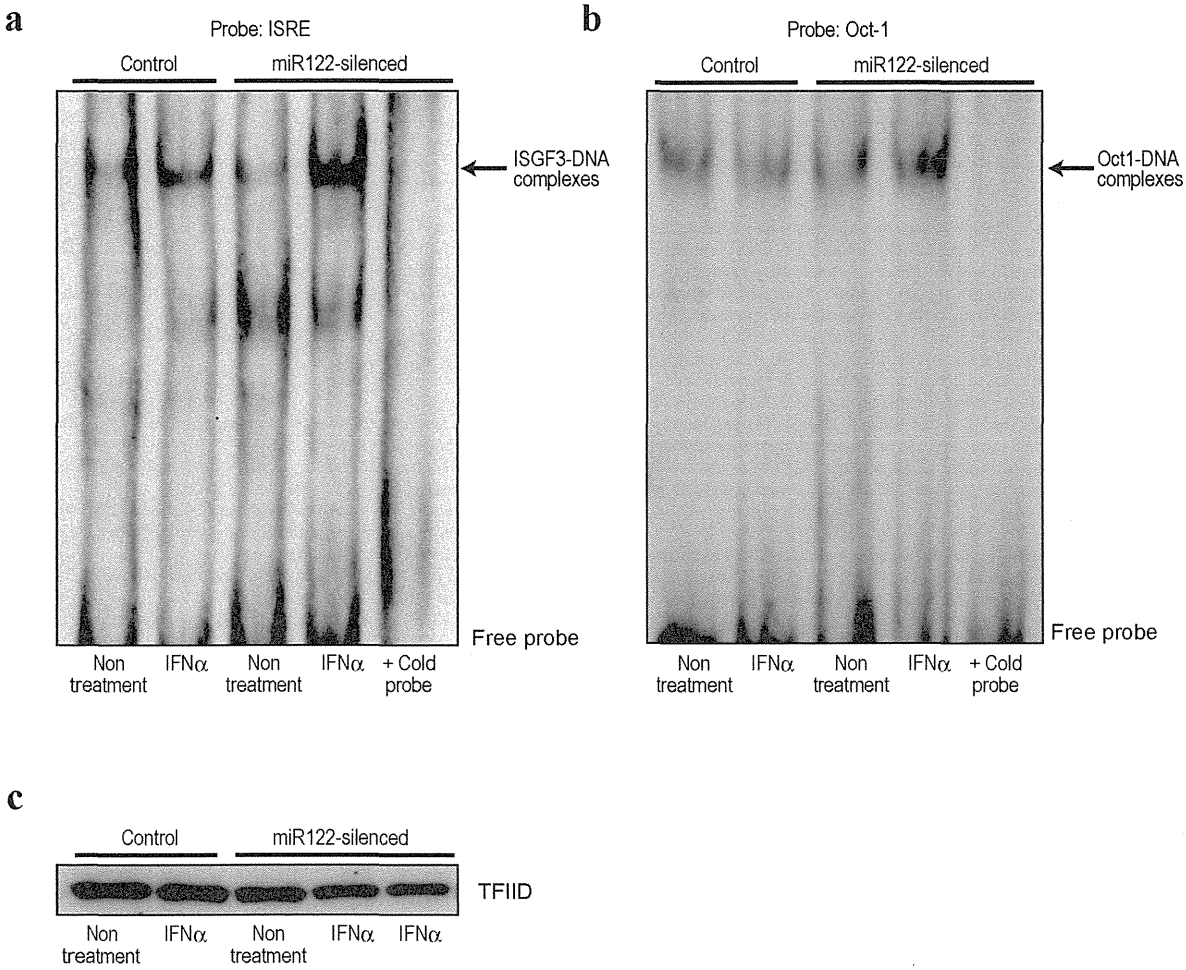

Figure 6 | ISGF3-ISRE DNA binding activity is increased in miR122-silenced cells. (a) DNA-binding ability of ISGF3 was determined by gel shift assay using ISRE consensus oligonucleotides. Nuclear extracts from control and miR122-silenced Huh7 cells with and without IFN-α stimulation for 1 h were used. Arrow indicates ISGF3-DNA complexes. The specificity of the DNA–protein complex was tested by adding unlabeled ISRE probe (cold probe) to IFN-α-stimulated miR122-silenced Huh7 nuclear extracts. A representative of three independent determinations is shown. (b) DNA-binding ability of Oct-1 was determined as a control for equal loading of nuclear extract. (c) TFIID amounts were examined by Western blotting to confirm equal nuclear extract loading. A representative of two independent determinations is shown.

Reagents. Human recombinant IFN-α, IFN-β, IFN-γ, and IL-28B (IFN-λ3) were purchased from R&D Systems (Minneapolis, MN) and used at final concentrations of 100 U/ml, 100 U/ml, 10 ng/mL, and 100 ng/mL, respectively. Doxycyclin and Tet-system fetal bovine serum were purchased from Clontech. Hygromycin was purchased from EMD Chemicals (Darmstadt, Germany).

Stable reporter cell lines and microRNA screening. To establish ISRE-luc reporter cell lines, 293T cells were transfected with the reporter plasmid pISRE-luc (Clontech) with a linear hygromycin resistance marker (Clontech). Single clones were selected in the presence of 250 μg/mL hygromycin. To screen for microRNAs that modulate ISRE activity, 75 microRNAs that are highly expressed in the liver[34], were reverse-transfected as described previously[15]. Briefly, synthetic mature microRNAs and, as a negative control, double-stranded RNA with artificial sequences (B-Bridge, Sapporo, Japan) were applied, with transfection reagents, to 96-well plates. The reporter cells were seeded to the plates, reverse-transfected, and then incubated for 48 h. ISRE-derived luciferase activity was measured using a GloMax 96 Microplate Luminometer (Promega, Madison, WI) after exposure to IFN-α for 12 h. Determinations were performed in duplicate, and the data were compared to those of the negative control.

Plasmids and tetracycline-inducible stable cell lines. The miR122 precursor expression plasmid was described previously[36]. The miR885 precursor expression plasmid was constructed by inserting a polymerase chain reaction (PCR)-generated 500 bp sequence encoding the miR885 precursor into the pCDH vector (System Biosciences, Mountain View, CA) using the *Xba*I and *Not*I sites. The resulting plasmid drives expression of miR885 under control of the CMV promoter. Plasmids expressing Halo-tagged SOCS3 were purchased from Promega. HA-tagged SOCS3 cDNA was amplified by PCR using the Halo-tagged SOCS3 plasmid as a template and the product was cloned into the pCDH-neo vector (System Biosciences) at the *Not*I site using In-fusion cloning method (Clontech). Plasmids expressing p53 were described previously[48]. To construct a tetracycline-regulated miR122 precursor expression plasmid, a PCR-amplified 500 bp region encoding themiR122 precursor was inserted into the pTRE2 vector (Clontech) using the *Bam*HI and *Sal*I sites. To establish tetracycline-regulated miR122 expressing stable cell lines, pTRE2miR122 plasmids were transfected into Hela-Tet-Off or Huh7-Tet-Off cell lines with a linear hygromycin marker (Clontech), followed by selection with hygromycin. Cells were cultured with or without 2.5 μg/ml doxycyclin. To establish SOCS3 overexpressing stable cells, HA-tagged SOCS3 expressing lentiviral particles were produced as described previously[36] and transduced into miR122-silenced Huh7 cells, followed by selection with G418 (Sigma, St. Louis, MO).

Lentiviral transduction. Huh7 cells were transduced with Dnmt1-shRNA and control-shRNA lentiviral particles (Santa Cruz Biotechnology, Santa Cruz, CA) and then selected on puromycin.

Western blot analysis and antibodies. Western blotting was performed as described previously[49]. All antibodies were purchased from Cell Signaling Technology (Danvers, MA), except anti-HA (Roche Applied Science, Indianapolis, IN) and anti-β-actin (Sigma).

Transfection and luciferase assay. Plasmid transfection was performed using FuGENE6 (Boehringer Mannheim, Mannheim, Germany) according to the manufacturer's protocol[36]. Luciferase activities were measured using a Dual Luciferase Reporter Assay System (Promega) as described previously[50].

Genome-wide DNA methylation analysis. Comprehensive DNA methylation analyses were performed by the outsourcing company MBL (Nagoya, Japan) using the Illumina Infinium methylation assay (Human Methylation27 BeadChip), which provides quantitative methylation levels at 27,578 promoter-associated CpG sites. Genomic DNA extracted from control and miR122-silenced Huh7 cells using QIAamp DNA mini kit (QIAGEN, Hilden, Germany) was used for this assay. Promoters with differential methylation levels were determined based on the standard criteria that differential values above 0.15 indicate significant differences in methylation status[51].

Bisulphite sequence analyses. Bisulphite sequence analyses were performed to check the methylation status of the SOCS3 promoter. Genomic DNA was extracted by QIAamp DNA mini kit (Qiagen) and bisulphate modified using MethylEasy Xceed Bisulphite Modification Kit (Human Genetic Signatures, North Ryde, Australia). The sequences of the SOCS3 promoter region were extracted as the upstream sequence of the transcriptional start site. The region of CpG islands and the PCR primers were determined using the web-based software MethPrimer[52]. PCR was performed using EpiTaq HS enzyme (TaKaRa, Shiga, Japan), according to the manufacturer's instructions. The PCR products were gel-purified using the QIAquick Gel Extraction Kit (Qiagen) and cloned into the TA vector using TOPO-TA cloning (Invitrogen). Seven clones from each sample were selected and the sequences were analyzed using a 3700 DNA analyzer (Applied Biosystems, Foster City, CA). The results were summarized using the web-based software, QUMA (http://quma.cdb.riken.jp/top/quma_main_j.html).

RNA extraction and quantitative RT-PCR analysis of microRNA expression levels. Total RNA was isolated from cells using Trizol Reagent (Invitrogen, Carlsbad, CA). To determine the levels of miR122 expression, cDNA was synthesized from RNA, and quantitative PCR was performed using an Mir-X miRNA First-Strand Synthesis and SYBR qRT-PCR Kit (Clontech). Relative expression values of microRNAs were calculated by the *CT*-based calibrated standard curve method. These values were then normalized to that of the U6 snRNA.

Electrophoretic mobility shift assay (EMSA). Nuclear extracts were prepared as described previously[53]. Five micrograms of nuclear extract were incubated with a double-stranded biotin-labeled DNA probe containing ISRE sites (5′-GAT CCA TGC CTC GGG AAA GGG AAA CCG AAA CTG AAG CC-3′)[54] or Oct-1 sites (Affymetrix, Santa Clara, CA) plus 1-μg poly (dI-dC) in a binding buffer (50 mM Tris [pH 7.5], 250 mM NaCl, 2.5 mM DTT, 2.5 mM EDTA, 5 mM $MgCl_2$, and 20% glycerol) at 15°C for 30 min. DNA–protein complexes were separated on 6% non-denaturing polyacrylamide gels in 0.5× TBE (25 mM Tris base, 24.25 mM boric acid, and 1 mM disodium EDTA) by electrophoresis at 120 V, 4°C for 30 min, and then transferred to Presoak Pall Biodyne B nylon membranes (Hybond-N^+; GE Healthcare Life Sciences) by electrophoresis in the same buffer for 30 min at 300 mA. Oligonucleotides were fixed using a UV cross-linker, and visualized using the LightShift Chemiluminescent EMSA Kit (Thermo Scientific, Rockford, IL), according to the manufacturers' instructions.

Statistical analysis. Statistically significant differences between groups were determined using Student's *t*-test when variances were equal. When variances were unequal, Welch's *t*-test was used. *P*-values less than 0.05 were considered statistically significant.

1. Hofmann, W. P. & Zeuzem, S. A new standard of care for the treatment of chronic HCV infection. *Nat Rev Gastroenterol Hepatol* **8**, 257–264 (2011).
2. Di Bisceglie, A. M. *et al.* Prolonged therapy of advanced chronic hepatitis C with low-dose peginterferon. *N Engl J Med* **359**, 2429–2441 (2008).
3. Hoofnagle, J. H. A step forward in therapy for hepatitis C. *N Engl J Med* **360**, 1899–1901 (2009).
4. Stetson, D. B. & Medzhitov, R. Type I interferons in host defense. *Immunity* **25**, 373–381 (2006).
5. Schindler, C. Teaching resources. Cytokine receptors and Jak-STAT signaling. *Sci STKE* **2006,** (2006).
6. Yoshimura, A., Naka, T. & Kubo, M. SOCS proteins, cytokine signalling and immune regulation. *Nat Rev Immunol* **7**, 454–465 (2007).
7. Funaoka, Y. *et al.* Analysis of interferon signaling by infectious hepatitis C virus clones with substitutions of core amino acids 70 and 91. *J Virol* **85**, 5986–5994 (2011).
8. Kim, K. A. *et al.* Hepatic SOCS3 expression is strongly associated with non-response to therapy and race in HCV and HCV/HIV infection. *J Hepatol* **50**, 705–711 (2009).
9. Miyaaki, H. *et al.* Predictive value of suppressor of cytokine signal 3 (SOCS3) in the outcome of interferon therapy in chronic hepatitis C. *Hepatol Res* **39**, 850–855 (2009).
10. Shao, R. X. *et al.* Suppressor of cytokine signaling 3 suppresses hepatitis C virus replication in an mTOR-dependent manner. *J Virol* **84**, 6060–6069 (2010).
11. Carrington, J. & Ambros, V. Role of microRNAs in plant and animal development. *Science* **301**, 336–338 (2003).
12. Bartel, D. P. MicroRNAs: genomics, biogenesis, mechanism, and function. *Cell.* **116**, 281–297 (2004).
13. Ambros, V. The functions of animal microRNAs. *Nature* **431**, 350–355 (2004).
14. Lu, J. *et al.* MicroRNA expression profiles classify human cancers. *Nature* **435**, 834–838 (2005).
15. Takata, A. *et al.* MicroRNA-22 and microRNA-140 suppress NF-κB activity by regulating the expression of NF-κB coactivators. *Biochem Biophys Res Commun* **411**, 826–831 (2011).
16. Park, S. Y., Lee, J. H., Ha, M., Nam, J. W. & Kim, V. N. miR-29 miRNAs activate p53 by targeting p85 alpha and CDC42. *Nat Struct Mol Biol* **16**, 23–29 (2009).
17. Kasinski, A. L. & Slack, F. J. Potential microRNA therapies targeting Ras, NFkappaB and p53 signaling. *Curr Opin Mol Ther* **12**, 147–157 (2010).
18. Ma, X., Becker Buscaglia, L. E., Barker, J. R. & Li, Y. MicroRNAs in NF-{kappa}B signaling. *J Mol Cell Biol* **3**, 159–166 (2011).
19. Hwang, H. W., Wentzel, E. A. & Mendell, J. T. A hexanucleotide element directs microRNA nuclear import. *Science* **315**, 97–100 (2007).
20. Wu, L. *et al.* DNA methylation mediated by a microRNA pathway. *Mol Cell* **38**, 465–47 (2010).
21. Sato, F., Tsuchiya, S., Meltzer, S. J. & Shimizu, K. MicroRNAs and epigenetics. *FEBS J* **278**, 1598–1609 (2011).
22. Fabbri, M. & Calin, G. A. Epigenetics and miRNAs in human cancer. *Adv Genet* **70**, 87–99 (2010).
23. Saetrom, P., Snøve, O. & Rossi, J. J. Epigenetics and microRNAs. *Pediatr Res* **61**, 17R–23R (2007).
24. Landgraf, P. *et al.* A mammalian microRNA expression atlas based on small RNA library sequencing. *Cell* **129**, 1401–1414 (2007).
25. Bhattacharyya, S., Habermacher, R., Martine, U., Closs, E. & Filipowicz, W. Relief of microRNA-mediated translational repression in human cells subjected to stress. *Cell* **125**, 1111–1124 (2006).
26. Esau, C. *et al.* miR-122 regulation of lipid metabolism revealed by in vivo antisense targeting. *Cell Metab* **3**, 87–98 (2006).
27. Li, E., Beard, C. & Jaenisch, R. Role for DNA methylation in genomic imprinting. *Nature* **366**, 362–365 (1993).
28. Brierley, M. M. & Fish, E. N. Stats: multifaceted regulators of transcription. *J Interferon Cytokine Res* **25**, 733–744 (2005).
29. Platanias, L. C. Mechanisms of type-I- and type-II-interferon-mediated signalling. *Nat Rev Immunol* **5**, 375–386 (2005).
30. Icardi, L. *et al.* Opposed regulation of type I IFN-induced STAT3 and ISGF3 transcriptional activities by histone deacetylases (HDACS) 1 and 2. *FASEB J* **26**, 240–9 (2011).
31. Ho, H. H. & Ivashkiv, L. B. Role of STAT3 in type I interferon responses. Negative regulation of STAT1-dependent inflammatory gene activation. *J Biol Chem* **281**, 14111–14118 (2006).
32. Gantier, M. P. New perspectives in MicroRNA regulation of innate immunity. *J Interferon Cytokine Res* **30**, 283–289 (2010).
33. David, M. Interferons and microRNAs. *J Interferon Cytokine Res* **30**, 825–828 (2010).
34. Krützfeldt, J. *et al.* Silencing of microRNAs in vivo with 'antagomirs'. *Nature* **438**, 685–689 (2005).
35. Gatfield, D. *et al.* Integration of microRNA miR-122 in hepatic circadian gene expression. *Genes Dev* **23**, 1313–1326 (2009).
36. Kojima, K. *et al.* MicroRNA122 is a key regulator of α-fetoprotein expression and influences the aggressiveness of hepatocellular carcinoma. *Nat Commun* **2**, 338 (2011).
37. Bartel, D. P. MicroRNAs: target recognition and regulatory functions. *Cell* **136**, 215–233 (2009).
38. Jopling, C., Yi, M., Lancaster, A., Lemon, S. & Sarnow, P. Modulation of hepatitis C virus RNA abundance by a liver-specific MicroRNA. *Science* **309,** (2005).
39. Lanford, R. E. *et al.* Therapeutic silencing of microRNA-122 in primates with chronic hepatitis C virus infection. *Science* **327**, 198–201 (2010).
40. Sheridan, C. New Merck and Vertex drugs raise standard of care in hepatitis C. *Nat Biotechnol* **29**, 553–554 (2011).
41. Pedersen, I. M. *et al.* Interferon modulation of cellular microRNAs as an antiviral mechanism. *Nature* **449**, 919–922 (2007).
42. Suppiah, V. *et al.* IL28B is associated with response to chronic hepatitis C interferon-alpha and ribavirin therapy. *Nat Genet* **41**, 1100–1104 (2009).
43. Tanaka, Y. *et al.* Genome-wide association of IL28B with response to pegylated interferon-alpha and ribavirin therapy for chronic hepatitis C. *Nat Genet* **41**, 1105–1109 (2009).
44. Pillai, R. S., Bhattacharyya, S. N. & Filipowicz, W. Repression of protein synthesis by miRNAs: how many mechanisms? *Trends Cell Biol.* **17**, 118–126 (2007).
45. Honda, M. *et al.* Hepatic ISG expression is associated with genetic variation in interleukin 28B and the outcome of IFN therapy for chronic hepatitis C. *Gastroenterology* **139**, 499–509 (2010).
46. Akuta, N. *et al.* Predictors of viral kinetics to peginterferon plus ribavirin combination therapy in Japanese patients infected with hepatitis C virus genotype 1b. *J Med Virol* **79**, 1686–1695 (2007).
47. Akuta, N. *et al.* Substitution of amino acid 70 in the hepatitis C virus core region of genotype 1b is an important predictor of elevated alpha-fetoprotein in patients without hepatocellular carcinoma. *J Med Virol* **80**, 1354–1362 (2008).
48. Dharel, N. *et al.* Potential contribution of tumor suppressor p53 in the host defense against hepatitis C virus. *Hepatology* **47**, 1136–1149 (2008).
49. Otsuka, M. *et al.* Hypersusceptibility to vesicular stomatitis virus infection in Dicer1-deficient mice is due to impaired miR24 and miR93 expression. *Immunity* **27**, 123–134 (2007).
50. Otsuka, M. *et al.* Impaired microRNA processing causes corpus luteum insufficiency and infertility in mice. *J Clin Invest* **118**, 1944–1954 (2008).

51. Bibikova, M. *et al.* Genome-wide DNA methylation profiling using Infinium assay. *Epigenomics* **1**, 177–200 (2009).
52. Li, L. C. & Dahiya, R. MethPrimer: designing primers for methylation PCRs. *Bioinformatics* **18**, 1427–1431 (2002).
53. Schreiber, E., Matthias, P., Müller, M. & Schaffner, W. Rapid detection of octamer binding proteins with 'mini-extracts', prepared from a small number of cells. *Nucleic Acids Res* **17**, 6419 (1989).
54. Wong, L. H., Hatzinisiriou, I., Devenish, R. J. & Ralph, S. J. IFN-gamma priming up-regulates IFN-stimulated gene factor 3 (ISGF3) components, augmenting responsiveness of IFN-resistant melanoma cells to type I IFNs. *J Immunol* **160**, 5475–5484 (1998).

Acknowledgments

This work was supported by Grants-in-Aid from the Ministry of Education, Culture, Sports, Science and Technology, Japan (#22390058, #24590956 and #20390204) (to M.O., H.Y. and K.Koike), by Health Sciences Research Grants of The Ministry of Health, Labour and Welfare of Japan (Research on Hepatitis) (to K.Koike) and grants from the Mochida Memorial Foundation for Medical and Pharmaceutical Research, the Yakult Bio-Science Foundation and the Cell Science Research Foundation (to M.O.).

Author contributions

T.Y., A.T., and M.O. planned the research and wrote the paper. T.Y., A.T., M.O., and T.K. performed the experiments. H.Y. analyzed the data. K.K. supervised the entire project.

Additional information

Competing financial interests: The authors declare no competing financial interests.

How to cite this article: Yoshikawa, T. *et al.* Silencing of microRNA-122 enhances interferon-α signaling in the liver through regulating SOCS3 promoter methylation. *Sci. Rep.* **2**, 637; DOI:10.1038/srep00637 (2012).

J Gastroenterol (2012) 47:187–194
DOI 10.1007/s00535-011-0477-8

ORIGINAL ARTICLE—LIVER, PANCREAS, AND BILIARY TRACT

Serum gamma-glutamyltransferase level is associated with serum superoxide dismutase activity and metabolic syndrome in a Japanese population

Hayato Nakagawa · Akihiro Isogawa · Ryosuke Tateishi · Mizuki Tani · Haruhiko Yoshida · Minoru Yamakado · Kazuhiko Koike

Received: 27 June 2011 / Accepted: 16 August 2011 / Published online: 6 October 2011

Abstract
Background Serum gamma-glutamyltransferase level has attracted considerable attention as a predictor of various conditions, such as cardiovascular disease and cancer. Although the mechanism that links the serum gamma-glutamyltransferase level to these diseases is not fully understood, one explanation is that gamma-glutamyltransferase may be closely related to oxidative stress. We conducted a large cross-sectional study to evaluate the relationship between serum gamma-glutamyltransferase and oxidative stress.
Methods We examined anti-oxidative stress activity and accumulation of oxidative stress in serum obtained from 2907 subjects who underwent a complete health check-up. We used serum total superoxide dismutase activity as an index of anti-oxidative stress activity. Superoxide dismutase is one of the most important intracellular and extracellular defense systems against superoxide, but the relationship between serum superoxide dismutase activity and the serum gamma-glutamyltransferase level is unclear.
Results The serum gamma-glutamyltransferase level was negatively correlated with serum superoxide dismutase activity, a correlation that was observed even within the normal range. A subgroup analysis stratified by the amount of alcohol consumed also showed a similar correlation. In contrast, the serum gamma-glutamyltransferase level was positively correlated with serum lipid peroxide level, even in the normal range. Furthermore, an increased serum gamma-glutamyltransferase level was significantly associated with the progression of metabolic syndrome and carotid artery intima-media thickness.
Conclusions The serum gamma-glutamyltransferase level, even in the normal range, was significantly associated with anti-oxidative stress activity, the accumulation of oxidative stress, metabolic syndrome, and atherosclerosis. Measuring the serum gamma-glutamyltransferase level is simple and inexpensive, and this level can be used as a sensitive marker of oxidative stress and metabolic syndrome.

Keywords Gamma-glutamyltransferase · Superoxide dismutase · Lipid peroxide · Metabolic syndrome · Atherosclerosis

Abbreviations

ALT	Alanine aminotransferase
BMI	Body mass index
CuZn-SOD	Copper/zinc-containing superoxide dismutase
DBP	Diastolic blood pressure
GGT	Gamma-glutamyltransferase
GSH	Glutathione
HDL-C	High-density lipoprotein-cholesterol
IMT	Intima-media thickness
ROS	Reactive oxygen species
SBP	Systolic blood pressure
TC	Total cholesterol
T-SOD	Total superoxide dismutase

H. Nakagawa (✉) · R. Tateishi · H. Yoshida · K. Koike
Department of Gastroenterology, University of Tokyo, 7-3-1 Hongo, Bunkyo-ku, Tokyo 113-8655, Japan
e-mail: n-hayato@yf7.so-net.ne.jp

H. Nakagawa · M. Tani · M. Yamakado
Center for Multiphasic Health Testing and Services, Mitsui Memorial Hospital, 1 Kanda-Izumi-cho, Chiyoda-ku, Tokyo 101-8643, Japan

A. Isogawa
Department of Internal Medicine, Mitsui Memorial Hospital, 1 Kanda-Izumi-cho, Chiyoda-ku, Tokyo 101-8643, Japan

Introduction

The serum gamma-glutamyltransferase (GGT) level has been widely used as an indicator of liver disease and alcohol consumption [1]. GGT has attracted considerable attention as a predictor of metabolic syndrome, insulin resistance, cardiovascular disease, stroke, and cancer [2–7]. Furthermore, elevated GGT is associated with higher all-cause mortality [8, 9].

The mechanism that links the serum GGT level to various diseases and mortality is not fully understood. One explanation is that GGT may be closely related to oxidative stress [10–12]. GGT is the enzyme responsible for the extracellular catabolism of glutathione (GSH), the main thiol intracellular antioxidant agent in most cells. Because GGT plays important roles in GSH homeostasis, GGT expression increases as an adaptive response upon exposure to oxidative stress. However, paradoxically, GGT is also directly involved in the generation of reactive oxygen species (ROS) under physiological conditions, particularly in the presence of iron or other transition metals [13]. Thus, the serum GGT level may reflect not only the response to oxidative stress, but also the generation and accumulation of oxidative stress. The serum GGT level has been associated with some oxidative stress markers, such as carotenoids, tocopherols, and lipid peroxide (LPO) [14–16].

Superoxide dismutase (SOD) exists in three isoforms: cytosolic copper/zinc-containing SOD (CuZn-SOD), mitochondrial manganese-containing SOD (Mn-SOD), and extracellular SOD [17, 18]. These enzymes contain redox metals in their catalytic centers and dismutate superoxide radicals to hydrogen peroxide and oxygen. SOD is an endogenous free-radical scavenger and one of the most important intracellular and extracellular defense systems against superoxide, an oxygen-derived free radical that has been implicated in various oxidative cell injuries. The measurement of serum total SOD (T-SOD) activity reflects systemic oxidative stress status, and its level is negatively correlated with atherosclerosis [19]. However, the relationship between serum T-SOD activity and the serum GGT level is unclear.

To evaluate the usefulness of the serum GGT level as an oxidative stress marker, we conducted a large cross-sectional study in 2907 subjects who underwent a complete health check-up. We used serum T-SOD and serum LPO levels as indexes of anti-oxidative stress activity and of the accumulation of oxidative stress, respectively. Additionally, to assess the clinical relevance of the serum GGT level, we investigated the association between the serum GGT level, metabolic syndrome, and carotid atherosclerosis.

Methods

Subjects

Between January 2001 and December 2003, 2907 subjects who had undergone general health screening tests, including carotid ultrasonography, at the Center for Multiphasic Health Testing Services, Mitsui Memorial Hospital, were enrolled. In Japan, regular employee health check-ups are mandated by law. Thus, the majority of these subjects had no major health problem. Blood samples were taken after an overnight fast. Data on hepatitis C core antigen and hepatitis B surface antigen were available in 2877 subjects (98.9%); 23 of these 2877 subjects were positive for hepatitis C and 40 were positive for hepatitis B. Because serum GGT levels did not differ between hepatitis-positive (48.0 ± 45.9 IU/L) and -negative (49.1 ± 57.8 IU/L) subjects, the hepatitis-positive subjects were not excluded.

Serum T-SOD activity was routinely determined with a computerized electron spin resonance spectrometer system (JES-FR30; JEOL, Tokyo, Japan) [19]. Serum LPO level was measured using the fluorimetric assay method of Yagi [20]. Carotid artery status was examined using a high-resolution B-mode ultrasonography instrument (Sonolayer SSA270A; Toshiba, Tokyo, Japan), equipped with a 7.5-MHz transducer (PLF-703ST; Toshiba). The carotid arteries were examined bilaterally at the level of the common carotid, the bifurcation, and the internal carotid arteries from transverse and longitudinal orientations. Carotid artery intima-media thickness (IMT) was measured, using a computer-assisted method, by experienced sonographers who were unaware of the subjects' clinical and laboratory findings.

Of the 2907 subjects, 2249 (77.3%) had undergone abdominal ultrasonography. All abdominal ultrasonography was performed with an SSD-5500 system (Aloka, Wallingford, CT, USA) and a 3.5-MHz convex probe. Fatty liver was diagnosed based on a bright liver with hepatorenal echo contrast.

This study was conducted after written informed consent was received from all subjects. The study protocol conformed to the ethical guidelines of the 1975 Declaration of Helsinki and was approved by the ethics committee of Mitsui Memorial Hospital (MEC2009-30).

Analysis

Body mass index (BMI) was calculated as the square of weight (in kg) divided by height (in meters). We defined obesity as BMI ≥ 25 kg/m^2, hypertension as systolic blood pressure ≥ 130 mmHg or diastolic blood pressure

≥85 mmHg, hypertriglyceridemia as a serum triglyceride concentration of ≥150 mg/dL, low high-density lipoprotein-cholesterol (HDL-C) as HDL-C ≤40 mg/dL for men or ≤50 mg/dL for women, and hyperglycemia as a fasting blood sugar level of ≥110 mg/dL. We defined the metabolic syndrome score as the number of these metabolic syndrome markers, based on the National Cholesterol Education Program Adult Treatment Program III definition.

Serum GGT levels were classified in sextiles; cut-off points of the sextiles for serum GGT were 16, 22, 31, 45, and 77 IU/L. We described the six categories defined by these cut-off points as categories A (serum GGT level ≤16 IU/L), B (17–22 IU/L), C (23–31 IU/L), D (32–45 IU/L), E (46–77 IU/L), and F (> 77 IU/L), respectively. We used sextile classification because we reasoned that the highest GGT group should consist of only the subjects with a serum GGT level above the upper normal limit at our institute (74 IU/L). In quartile and quintile classifications, the highest cut-off point of GGT did not exceed the upper normal limit (58 and 65 IU/L, respectively).

Statistical analyses

Data are expressed as means ± standard deviations. Correlations between variables were analyzed using Spearman's rank correlation coefficient. Stepwise multiple linear regression analysis was used to identify variables that were independently related to serum T-SOD activity. Trends in serum T-SOD activity, LPO level, metabolic score, and IMT in relation to serum GGT levels were assessed with the Jonckheere-Terpstra test. Continuous variables were compared with the unpaired Student's *t*-test (parametric) or the Mann–Whitney *U*-test (nonparametric). A *P* value of <0.05 on a two-tailed test was considered statistically significant. Data processing and analyses were performed using StatView (ver. 5.0; SAS Institute, Cary, NC, USA) and SPSS (ver. 14.0; SPSS, Chicago, IL, USA) software.

Results

Subjects' characteristics

The subjects' characteristic are shown in Table 1. The frequencies of hyperglycemia, hypertension, hypertriglyceridemia, low-HDL-cholesterolemia, and obesity were 14.0, 38.1, 26.0, 8.1, and 27.3%, respectively.

Correlation between serum T-SOD activity and GGT level

To assess whether serum T-SOD activity was linked to metabolic syndrome, we investigated the correlations between serum T-SOD activity and clinical parameters associated with metabolic syndrome. Our results revealed significant correlations between serum T-SOD activity and various clinical parameters that tended to decline with the progression of metabolic syndrome, although these correlations were generally weak (Table 2). Of these parameters, serum GGT was most strongly correlated with serum T-SOD activity ($\rho = -0.16$, $P < 0.0001$). To identify variables that were independently related to serum T-SOD activity, we performed multiple linear regression analysis. Serum T-SOD activity could be predicted by serum GGT, HDL-C, alanine aminotransferase (ALT), age, fasting

Table 1 Baseline characteristics

Variables	$n = 2907$
Age (years)	55.2 ± 10.8
Sex (male/female)	1896/1017
BMI (kg/m^2)	23.3 ± 3.1
SBP (mmHg)	124.4 ± 19.2
DBP (mmHg)	77.7 ± 11.7
TC (mg/dL)	209 ± 34.6
HDL-C (mg/dL)	62.1 ± 16.4
TG (mg/dL)	128 ± 115.2
Glucose (mg/dL)	98.9 ± 21.3
Insulin (IU/L)	6.1 ± 3.8
GGT (IU/L)	49.2 ± 57.6
ALT (IU/L)	27.0 ± 31.1
T-SOD (U/ml)	2.9 ± 1.2
LPO (nmol/ml)	0.8 ± 0.9

BMI Body mass index, *SBP* systolic blood pressure, *DBP* diastolic blood pressure, *TC* total cholesterol, *HDL-C* high-density lipoprotein-cholesterol, *TG* triglycerides, *GGT* gamma-glutamyltransferase, *ALT* alanine aminotransferase, *T-SOD* total superoxide dismutase, *LPO* lipid peroxide

Table 2 Correlations between serum T-SOD activity and other parameters

Variables	Spearman's rho	*P*
Age	0.086	<0.0001
BMI	−0.15	<0.0001
SBP	−0.086	<0.0001
DBP	−0.094	<0.0001
TC	0.06	0.011
HDL-C	0.146	<0.0001
TG	−0.129	<0.0001
Glucose	−0.136	<0.0001
Insulin	−0.125	<0.0001
GGT	−0.16	<0.0001
ALT	−0.071	0.0001

blood sugar, and systolic blood pressure, and standardized beta coefficients showed that, of these parameters, serum GGT had the strongest influence on T-SOD activity (Table 3). From these results, we considered that the serum GGT level was an independent and important predictor of serum T-SOD activity, although the correlation was weak. Interestingly, in the ordered categorical analysis using sextiles, serum T-SOD activity declined in a stepwise fashion even within the normal range of the serum GGT level ($P < 0.0001$; Fig. 1a).

Correlation between serum LPO and GGT level

Next, we assessed the correlation between serum GGT and the serum LPO level, which was used as a representative marker for oxidative stress accumulation. In contrast to the serum T-SOD activity, the serum LPO level increased in a stepwise fashion even within the normal range of the serum GGT level ($P < 0.0001$; Fig. 1b). Thus, the serum GGT level closely reflected both anti-oxidative stress activity and the accumulation of oxidative stress.

Table 3 Multiple linear regression analysis using serum T-SOD activity as dependent variable

Variables	Standardized beta	*P*
Age	0.077	<0.0001
BMI		NS
SBP	−0.045	0.023
DBP		NS
TC		NS
HDL-C	0.096	<0.0001
TG		NS
Glucose	−0.057	0.003
Insulin		NS
GGT	−0.112	<0.0001
ALT	−0.057	0.003

NS Not significant

Correlation of serum GGT level with metabolic syndrome and IMT

To assess the clinical relevance of serum GGT levels, we investigated the correlation of the serum GGT level with the metabolic score and IMT. Similar to oxidative stress, the metabolic score also increased in a stepwise fashion, even within the normal range of the serum GGT level ($P < 0.0001$; Fig. 2). Furthermore, the serum GGT level was significantly and positively correlated with IMT ($P < 0.0001$; Fig. 3). Thus, an increased serum GGT level was associated with the metabolic syndrome and atherosclerosis.

Influence of drinking status on the relationship of the serum GGT level to serum SOD activity and metabolic syndrome

The serum GGT level is known to be influenced by the amount of alcohol consumed. To investigate the influence of drinking status on the relationship of the serum GGT level to SOD activity and the metabolic syndrome, we stratified subjects into four groups according to the amount of alcohol consumed: never ($n = 1053$), 1–30 g/day ($n = 886$), 31–60 g/day ($n = 631$), and >60 g/day ($n = 337$). As shown in Fig. 4a, the serum GGT level showed a significant positive graded association with the amount of alcohol consumed. T-SOD activity was negatively correlated with the amount of alcohol consumed and the metabolic score was positively correlated with this parameter (Fig. 4b, c). These findings suggest that drinking status may confound the relationship of the serum GGT level to T-SOD activity and the metabolic syndrome. Therefore, to rule out the influence of drinking status, we re-analyzed these relationships after stratifying the sample based on the amount of alcohol consumed. As shown in Fig. 4d, the serum GGT level showed a significant negative correlation with serum T-SOD activity in all subgroups stratified by drinking status. Furthermore, the serum GGT level showed

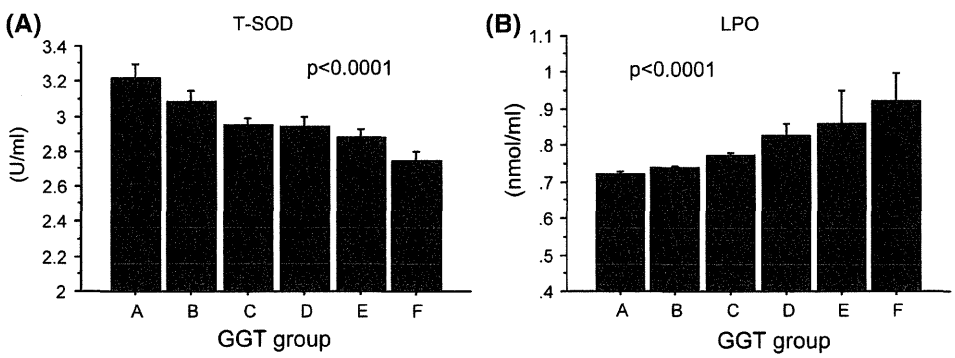

Fig. 1 Relationship of serum gamma-glutamyltransferase (*GGT*) level to serum total superoxide dismutase (*T-SOD*) activity and lipid peroxide level. *Bar graph* shows serum T-SOD activity (**a**) and lipid peroxide (*LPO*) level (**b**) according to sextiles of serum GGT level

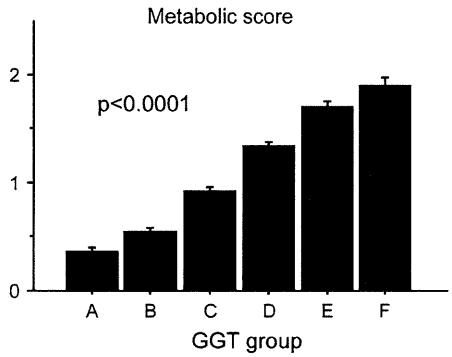

Fig. 2 Correlation between serum GGT level and metabolic syndrome. *Bar graph* shows metabolic score according to sextiles of serum GGT level

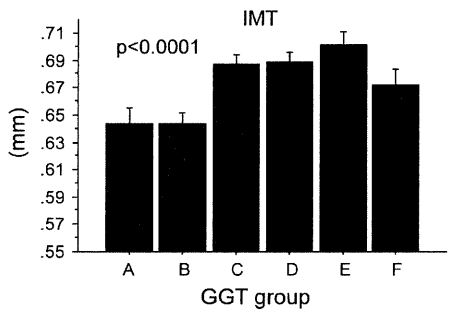

Fig. 3 Correlation between serum GGT level and atherosclerosis. *Bar graph* shows intima-media thickness (*IMT*) according to sextiles of serum GGT level

a clear positive correlation with the metabolic score in all subgroups (Fig. 4e). These results suggest that the serum GGT level was correlated with serum T-SOD activity and the metabolic syndrome, independent of drinking status.

Gender-separated analysis

Because there is a gender difference in serum GGT levels, we performed a gender-separated analysis to identify correlations among serum GGT level, oxidative stress, and the metabolic syndrome. The serum GGT level was more strongly correlated with oxidative stress in males than in females (Fig. 5a, b). In contrast, the metabolic score showed similar positive correlations with the serum GGT level in both genders (Fig. 5c).

Influence of fatty liver on the relationship between serum GGT and serum SOD activity

Because the serum GGT level is also affected by the presence of fatty liver [9], we assessed the influence of fatty liver on the relationship between serum GGT and serum SOD activity. Among the 2249 subjects who underwent abdominal ultrasonography, a fatty liver was found in 652 (28.9%). The serum GGT level was significantly higher in subjects with a fatty liver (66.9 ± 76.2 IU/L) than in subjects without a fatty liver (46.3 ± 51.2 IU/L; $P < 0.0001$). However, serum T-SOD activity was significantly lower in subjects with a fatty liver (2.84 ± 1.08 U/mL) than in subjects without a fatty liver (3.00 ± 1.30 U/mL; $P = 0.007$), suggesting that the presence of fatty liver was associated with decreased serum T-SOD activity. Next, we conducted a subgroup analysis for the correlation between serum GGT and serum SOD activity, stratified according to the presence of fatty liver. Subjects without a fatty liver showed a significant negative correlation between the serum GGT level and serum SOD activity ($\rho = -0.158$, $P < 0.0001$), whereas subjects with a fatty liver showed a similar but statistically insignificant tendency toward a negative correlation ($\rho = -0.067$, $P = 0.08$). Thus, the presence of fatty liver may have partially confounded the relationship between the serum GGT level and serum T-SOD activity.

Discussion

In the present study, by analyzing a large dataset of subjects who underwent general health screening, we found that serum GGT levels, even within the normal range, closely reflected oxidative stress and metabolic syndrome. To our knowledge, this is the first report describing the relationship between serum GGT level and serum T-SOD activity.

GGT increases as an adaptive response upon exposure to oxidative stress, and GGT metabolizes extracellular GSH to provide component amino acids for intracellular GSH resynthesis [10–12]. GSH protects cells from oxidative stress by reacting with hydrogen peroxide, superoxide anions, singlet oxygen, and hydroxyl radicals [21]. GSH has been implicated in protection against ROS-mediated cell death in a variety of cell types [21, 22]. Thus, a higher serum GGT level may reflect chronic depletion of intracellular GSH due to the high accumulation of oxidative stress, which can lead to various diseases.

GGT is directly involved in ROS generation. This concept is based on the experimental findings that cysteinylglycine, a product of GGT action on GSH, has a strong ability to reduce Fe^{3+} to Fe^{2+}, which promotes ROS generation [13]. Furthermore, GGT-generated glutathione hydrolysis triggers iron-catalyzed LDL oxidation, which promotes plaque [23]. In fact, the serum GGT level was significantly correlated with carotid artery IMT in our study. However, IMT in group F, which had the highest serum GGT, was slightly decreased compared with results in groups C–E (Fig. 4). This finding may have been

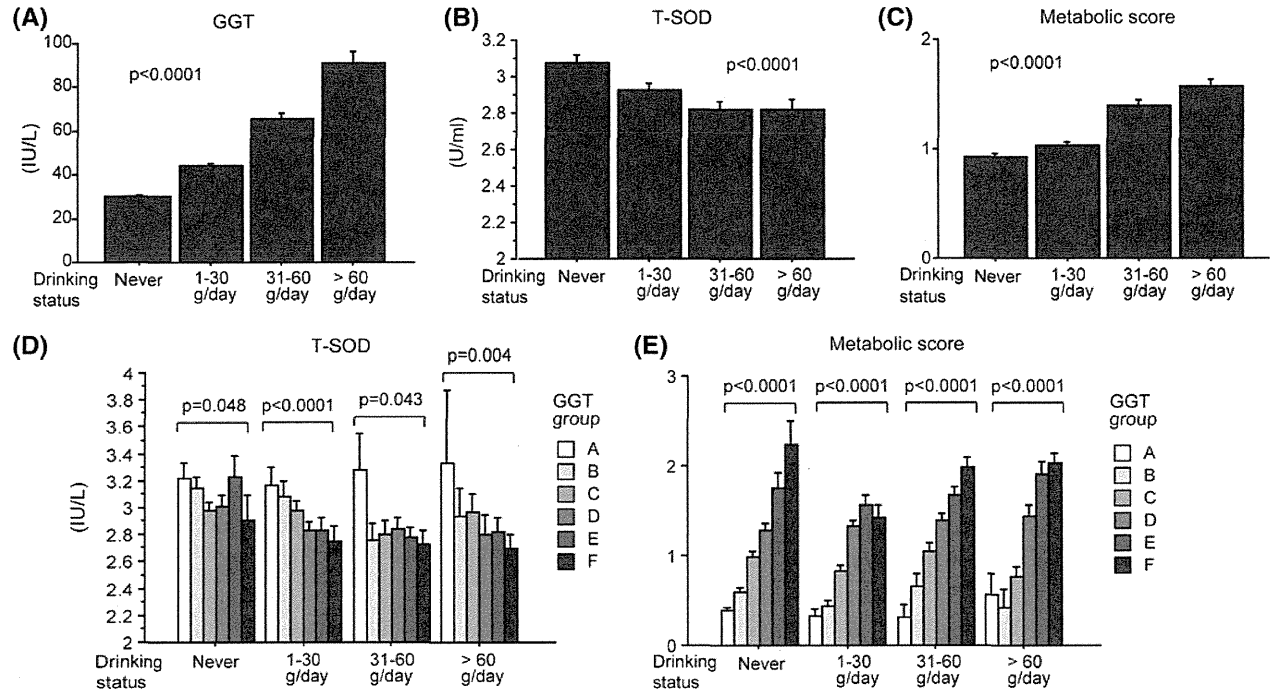

Fig. 4 Influence of drinking status on the relationship of serum GGT level to serum T-SOD activity and metabolic syndrome. Influence of drinking status on serum GGT level, serum T-SOD activity, and metabolic score is shown. *Bar graph* shows serum GGT level (**a**), serum T-SOD activity (**b**), and metabolic score (**c**) according to drinking status. *Bar graph* also shows the correlation between serum GGT and serum T-SOD activity (**d**), and the correlation between serum GGT and metabolic score (**e**) stratified by drinking status

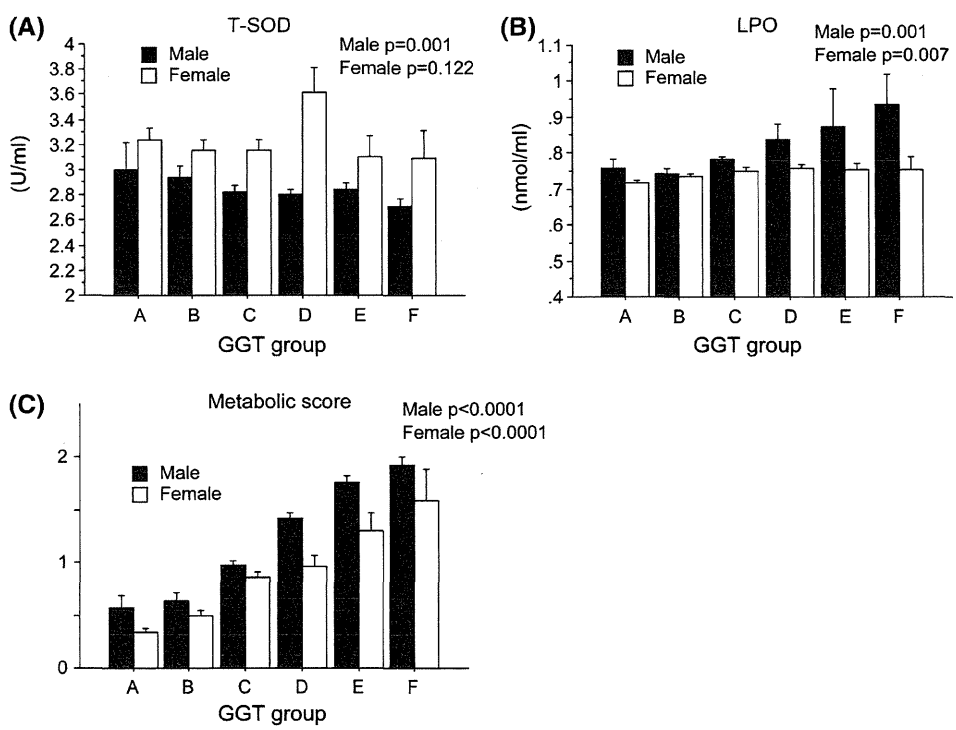

Fig. 5 Gender separated analysis of serum GGT level as the marker of oxidative stress and metabolic syndrome. *Bar graph* shows (**a**) serum T-SOD level, (**b**) serum lipid peroxide level, and (**c**) metabolic score according to sextiles of serum GGT level

confounded by the protective effect of moderate alcohol consumption on atherosclerosis.

Our finding that serum GGT was negatively correlated with serum T-SOD activity suggests that decreased anti-oxidative stress activity may link the serum GGT level to the progression of various diseases. Serum SOD is the first-line anti-oxidant enzyme defense system, particularly for the endothelium against extracellular ROS, which initiate processes involved in atherogenesis [24, 25]. Thus, GGT may be involved not only in intracellular oxidative stress through GSH synthesis, but also in extracellular oxidative stress by modulating SOD expression. A previous report showed that CuZn-SOD mRNA was upregulated in GGT mutant mice [26], suggesting that GGT may be directly correlated with SOD activity. However, in our study, a subgroup analysis according to the presence of fatty liver indicated that a fatty liver may have partially confounded the relationship between the serum GGT level and serum T-SOD activity. CuZn-SOD-deficient mice have been shown to exhibit lipid accumulation in the liver, suggesting that decreased SOD activity may lead to fatty liver, which may induce an elevation of serum GGT levels [27]. From the present type of cross-sectional study, we cannot conclude whether there is a causal relationship between GGT and SOD activity, so further study is needed. We can at least say that decreased anti-oxidative stress activity may be linked to the serum GGT level and various diseases.

Our gender-separated analysis revealed that the serum GGT level was more strongly correlated with oxidative stress in males than in females. Although we cannot clarify the cause of this difference from this study, this finding may be interesting from the point of view of gender differences in the anti-oxidative stress defense system.

Our study has some limitations. First, we did not take into account the amount of coffee intake, which might affect GGT levels and oxidative stress [28]. Second, as mentioned above, our cross-sectional study design could not identify causal relationships among GGT, SOD activity, and metabolic syndrome. These relationships may be based on genetic background; for example, a single nucleotide polymorphism of SOD genes, or may simply represent a reactive phenomenon against ROS accumulation. Third, we did not exclude subjects who were taking antihypertensive and/or antidiabetic drugs, and this lack of exclusion could potentially affect the results of our study. In addition, we did not have sufficient information about the ingestion of anti-oxidative supplements that may have reduced the level of serum oxidative stress markers.

In conclusion, we showed that the serum GGT level, even within the normal range, was significantly associated with anti-oxidative stress activity, the accumulation of oxidative stress, the metabolic syndrome, and atherosclerosis. Measurement of the serum GGT level is simple and inexpensive, and it can be used as a sensitive marker of oxidative stress and metabolic syndrome. Furthermore, we should consider serum GGT levels during health examinations, even when these levels are within the normal range.

Acknowledgments This work was supported by Grants-in-Aid from the Ministry of Health, Labour and Welfare of Japan (H20-kannenn-008).

Conflict of interest None.

References

1. Whitfield JB. Gamma glutamyl transferase. Crit Rev Clin Lab Sci. 2001;38:263–355.
2. Giral P, Jacob N, Dourmap C, Hansel B, Carrie A, Bruckert E, et al. Elevated gamma-glutamyltransferase activity and perturbed thiol profile are associated with features of metabolic syndrome. Arterioscler Thromb Vasc Biol. 2008;28:587–93.
3. Ishizaka N, Ishizaka Y, Toda E, Yamakado M, Koike K, Nagai R. Association between gamma-glutamyltransferase levels and insulin resistance according to alcohol consumption and number of cigarettes smoked. J Atheroscler Thromb. 2010;17:476–85.
4. Fraser A, Harris R, Sattar N, Ebrahim S, Smith GD, Lawlor DA. Gamma-glutamyltransferase is associated with incident vascular events independently of alcohol intake: analysis of the British Women's Heart and Health Study and Meta-Analysis. Arterioscler Thromb Vasc Biol. 2007;27:2729–35.
5. Shimizu Y, Imano H, Ohira T, Kitamura A, Kiyama M, Okada T, et al. Gamma-glutamyltranspeptidase and incident stroke among Japanese men and women: the Circulatory Risk in Communities Study (CIRCS). Stroke. 2010;41:385–8.
6. Strasak AM, Rapp K, Brant LJ, Hilbe W, Gregory M, Oberaigner W, et al. Association of gamma-glutamyltransferase and risk of cancer incidence in men: a prospective study. Cancer Res. 2008;68:3970–7.
7. Strasak AM, Pfeiffer RM, Klenk J, Hilbe W, Oberaigner W, Gregory M, et al. Prospective study of the association of gamma-glutamyltransferase with cancer incidence in women. Int J Cancer. 2008;123:1902–6.
8. Lee DS, Evans JC, Robins SJ, Wilson PW, Albano I, Fox CS, et al. Gamma glutamyl transferase and metabolic syndrome, cardiovascular disease, and mortality risk: the Framingham Heart Study. Arterioscler Thromb Vasc Biol. 2007;27:127–33.
9. Haring R, Wallaschofski H, Nauck M, Dorr M, Baumeister SE, Volzke H. Ultrasonographic hepatic steatosis increases prediction of mortality risk from elevated serum gamma-glutamyl transpeptidase levels. Hepatology. 2009;50:1403–11.
10. Pompella A, Corti A, Paolicchi A, Giommarelli C, Zunino F. Gamma-glutamyltransferase, redox regulation and cancer drug resistance. Curr Opin Pharmacol. 2007;7:360–6.
11. Zhang H, Forman HJ. Redox regulation of gamma-glutamyl transpeptidase. Am J Respir Cell Mol Biol. 2009;41:509–15.
12. Lee DH, Jacobs DR Jr. Is serum gamma-glutamyltransferase a marker of exposure to various environmental pollutants? Free Radic Res. 2009;43:533–7.
13. Drozdz R, Parmentier C, Hachad H, Leroy P, Siest G, Wellman M. Gamma-glutamyltransferase dependent generation of reactive oxygen species from a glutathione/transferrin system. Free Radic Biol Med. 1998;25:786–92.
14. Lee DH, Gross MD, Jacobs DR Jr. Association of serum carotenoids and tocopherols with gamma-glutamyltransferase:

the Cardiovascular Risk Development in Young Adults (CARDIA) Study. Clin Chem. 2004;50:582–8.
15. Lim JS, Yang JH, Chun BY, Kam S, Jacobs DR Jr, Lee DH. Is serum gamma-glutamyltransferase inversely associated with serum antioxidants as a marker of oxidative stress? Free Radic Biol Med. 2004;37:1018–23.
16. Yamada J, Tomiyama H, Yambe M, Koji Y, Motobe K, Shiina K, et al. Elevated serum levels of alanine aminotransferase and gamma glutamyltransferase are markers of inflammation and oxidative stress independent of the metabolic syndrome. Atherosclerosis. 2006;189:198–205.
17. Zelko IN, Mariani TJ, Folz RJ. Superoxide dismutase multigene family: a comparison of the CuZn-SOD (SOD1), Mn-SOD (SOD2), and EC-SOD (SOD3) gene structures, evolution, and expression. Free Radic Biol Med. 2002;33:337–49.
18. Faraci FM, Didion SP. Vascular protection: superoxide dismutase isoforms in the vessel wall. Arterioscler Thromb Vasc Biol. 2004; 24:1367–73.
19. Isogawa A, Yamakado M, Yano M, Shiba T. Serum superoxide dismutase activity correlates with the components of metabolic syndrome or carotid artery intima-media thickness. Diabetes Res Clin Pract. 2009;86:213–8.
20. Yagi K. Assay for blood plasma or serum. Methods Enzymol. 1984;105:328–31.
21. Franco R, Schoneveld OJ, Pappa A, Panayiotidis MI. The central role of glutathione in the pathophysiology of human diseases. Arch Physiol Biochem. 2007;113:234–58.
22. Nakagawa H, Maeda S, Hikiba Y, Ohmae T, Shibata W, Yanai A, et al. Deletion of apoptosis signal-regulating kinase 1 attenuates acetaminophen-induced liver injury by inhibiting c-Jun N-terminal kinase activation. Gastroenterology. 2008;135:1311–21.
23. Paolicchi A, Minotti G, Tonarelli P, Tongiani R, De Cesare D, Mezzetti A, et al. Gamma-glutamyl transpeptidase-dependent iron reduction and LDL oxidation—a potential mechanism in atherosclerosis. J Investig Med. 1999;47:151–60.
24. Harrison D, Griendling KK, Landmesser U, Hornig B, Drexler H. Role of oxidative stress in atherosclerosis. Am J Cardiol. 2003;91:7A–11A.
25. Nishikawa T, Kukidome D, Sonoda K, Fujisawa K, Matsuhisa T, Motoshima H, et al. Impact of mitochondrial ROS production on diabetic vascular complications. Diabetes Res Clin Pract. 2007; 77(Suppl 1):S41–5.
26. Jean JC, Harding CO, Oakes SM, Yu Q, Held PK, Joyce-Brady M. Gamma-glutamyl transferase (GGT) deficiency in the GGTenu1 mouse results from a single point mutation that leads to a stop codon in the first coding exon of GGT mRNA. Mutagenesis. 1999;14:31–6.
27. Uchiyama S, Shimizu T, Shirasawa T. CuZn-SOD deficiency causes ApoB degradation and induces hepatic lipid accumulation by impaired lipoprotein secretion in mice. J Biol Chem. 2006;281:31713–9.
28. Poikolainen K, Vartiainen E. Determinants of gamma-glutamyltransferase: positive interaction with alcohol and body mass index, negative association with coffee. Am J Epidemiol. 1997;146: 1019–24.

Research Article

EASL EUROPEAN ASSOCIATION FOR THE STUDY OF THE LIVER | JOURNAL OF HEPATOLOGY

Increased activity of serum mitochondrial isoenzyme of creatine kinase in hepatocellular carcinoma patients predominantly with recurrence

Yoko Soroida[1,†], Ryunosuke Ohkawa[1,†], Hayato Nakagawa[1,2], Yumiko Satoh[1], Haruhiko Yoshida[2], Hiroto Kinoshita[2], Ryosuke Tateishi[2], Ryota Masuzaki[2], Kenichiro Enooku[1,2], Shuichiro Shiina[2], Takahisa Sato[3], Shuntaro Obi[3], Tadashi Hoshino[4], Ritsuko Nagatomo[1], Shigeo Okubo[1], Hiromitsu Yokota[1], Kazuhiko Koike[2], Yutaka Yatomi[1], Hitoshi Ikeda[1,2,*]

[1]*Department of Clinical Laboratory Medicine, Graduate School of Medicine, The University of Tokyo, 7-3-1 Hongo, Bunkyo-ku, Tokyo 113-8655, Japan;* [2]*Department of Gastroenterology, Graduate School of Medicine, The University of Tokyo, 7-3-1 Hongo, Bunkyo-ku, Tokyo 113-8655, Japan;* [3]*Department of Hepatology, Kyoundo Hospital, 1-8 Kandasurugadai, Chiyoda-ku, Tokyo 101-0062, Japan;* [4]*Division of Laboratory Medicine, Department of Pathology and Microbiology, Nihon University School of Medicine, 30-1 Oyaguchi-kamimachi, Itabashi-ku, Tokyo 173-8610, Japan*

Background & Aims: Mitochondrial isoenzyme of creatine kinase (MtCK) is reportedly highly expressed in hepatocellular carcinoma (HCC). Clinical relevance of serum MtCK activity in patients with HCC was assessed using a novel immuno-inhibition method.
Methods: Among patients with cirrhosis caused by hepatitis B or C virus, 147 patients with HCC (12 with the first occurrence and 135 with recurrence) and 92 patients without HCC were enrolled.
Results: Serum MtCK activity was higher in cirrhotic patients with HCC than in those without HCC or healthy subjects. Elevated serum MtCK activity in HCC patients decreased after radiofrequency ablation. In case of prediction of HCC, MtCK had a sensitivity of 62.6% and a specificity of 70.7% at a cut-off point of 8.0 U/L, with an area under the receiver operating curve of 0.722 *vs.* 0.713 for alpha-fetoprotein (AFP) and 0.764 for des-gamma-carboxy prothrombin (DCP). Among the HCC patients, serum MtCK activity was elevated in 52.9% individuals with serum AFP level <20 ng/ml and 63.2% individuals with serum DCP level <40 mAu/ml. Even in patients with a single HCC ⩽2 cm, the sensitivity of serum MtCK activity for the prediction of HCC was 64.4%, which was comparable to the overall sensitivity. This increased activity was due to an increase in ubiquitous MtCK, not sarcomeric MtCK, and the enhanced mRNA expression of ubiquitous MtCK was observed in cell lines originating from HCCs in contrast to healthy liver tissues.
Conclusions: Serum MtCK activity merits consideration as a novel marker for HCC to be further tested as for its diagnostic and prognostic power.

Introduction

Hepatocellular carcinoma (HCC) is a common malignancy worldwide [1]. Its incidence is currently increasing in many countries [2,3], and it usually develops in the setting of chronic liver injury [3]. Because liver cirrhosis is the strongest risk factor for HCC development, patients with cirrhosis require cancer surveillance. Given the improvements in the overall survival of patients with cirrhosis [4] and the increasing incidence of HCC in many countries, effective strategies for the early detection of HCC are urgently needed, since the prognosis of HCC is deemed poor unless the cancer can be detected and treated at an early stage [5].

Alpha-fetoprotein (AFP) has been the most widely used serum marker for HCC surveillance [5]. Prospective studies assessing AFP as a surveillance tool indicate a sensitivity of 39–64%, a specificity of 76–91%, and a positive predictive value of 9–32% for early HCC [6–8]. Des-gamma-carboxy prothrombin (DCP) is also a specific marker for HCC, but its sensitivity is not sufficiently high, even when combined with AFP [9–11]. Liver ultrasound reportedly has a sensitivity of 78%, a specificity of 91%, and a positive predictive value of 73% for the detection of early HCC [12]. However, the accuracy of ultrasound is operator-dependent, limiting its value as a surveillance test [13]. Thus, additional markers for HCC are still needed.

Keywords: Mitochondrial isoenzyme of creatine kinase; Hepatocellular carcinoma; Alpha-fetoprotein; Des-gamma-carboxy prothrombin.
Received 17 June 2011; received in revised form 6 March 2012; accepted 6 March 2012; available online 17 April 2012
* Corresponding author. Address: Department of Clinical Laboratory Medicine, Graduate School of Medicine, The University of Tokyo, 7-3-1 Hongo, Bunkyo-ku, Tokyo 113-8655, Japan. Tel.: +81 3 3815 5411; fax: +81 3 5689 0495.
E-mail address: ikeda-1im@h.u-tokyo.ac.jp (H. Ikeda).
† The authors contributed equally to this work.
Abbreviations: HCC, hepatocellular carcinoma; AFP, alpha-fetoprotein; DCP, des-gamma-carboxy prothrombin; CK, creatine kinase; MtCK, mitochondrial isoenzyme of creatine kinase; HBV, hepatitis B virus; HCV, hepatitis C virus; CK-MB, MB fraction of creatine kinase; CK-M, MM fraction of creatine kinase; RFA, radiofrequency ablation; APRI, aspartate aminotransferase-to-platelet ratio index; BCLC, Barcelona Clinic Liver Cancer.

Creatine kinase (CK) is a central controller of cellular energy homeostasis. By reversible interconversion of creatine into phosphocreatine, CK builds up a large pool of rapidly diffusing phosphocreatine for temporal and spatial buffering of ATP levels. Thus, CK plays a particularly important role in tissues with large and fluctuating energy demands, such as muscle and brain, and the mitochondrial isoenzyme of CK (MtCK) has been assumed to be important for the energetics of oxidative tissues [14], suggesting that MtCK also plays a pivotal role in malignant tissues. Indeed, overexpression of MtCK has been reported in malignant liver tissue [15], and the increased activity of serum MtCK has been reported in patients with malignant tumors including hepatic cancer, gastric cancer, and lung cancer [16]. Furthermore, the elevated activity of MtCK was recently determined in tissue samples of HCC [17]. These findings suggest that MtCK activity may be useful as a serum marker for HCC. However, Castaldo *et al.* reported that serum MtCK activity was detected in only 16% of HCC patients [18].

In these previous studies, serum MtCK level was measured using electrophoresis and densitometry [16,18]. On the other hand, a novel method for directly determining the enzymatic activity of MtCK has been recently established [19], and this method may have a better sensitivity and accuracy for the measurement of MtCK activity than the previous method. In the present study, we sought to examine the status of serum MtCK activity in patients with HCC using this novel method.

Patients and methods

Subjects

Consecutive HCC patients with cirrhosis caused by hepatitis B virus (HBV) or hepatitis C virus (HCV), who were treated at the Department of Gastroenterology, of the University of Tokyo Hospital, Tokyo, Japan, between January and April 2010, were enrolled (n = 147). Patients with cirrhosis caused by HBV or HCV but who did not have HCC (n = 92) were also enrolled. Diagnosis of cirrhosis was based on the presence of clinical and laboratory features indicating portal hypertension (the presence of esophageal varices and/or collateral circulation as observed using endoscopy, ultrasonography, CT or MRI). The diagnosis of HCC was made by dynamic CT or MRI [20], with hyperattenuation during the arterial phase and washout during the late phase regarded as definite signs of HCC [21]. The absence of HCC was determined by surveillance ultrasonography or by dynamic CT or MRI. Blood samples were drawn within one month after the diagnosis and prior to the initiation of treatment in HCC patients. In non-HCC patients, blood samples were obtained within one month since the last surveillance imaging, and the absence of HCC was confirmed at least 6 months after the analysis of blood samples. Whole blood specimens were also obtained from 61 healthy controls without liver damage.

In addition, HCC patients with cirrhosis and advanced lesions, i.e., a maximum diameter of 6 cm or larger, diffuse liver lesions, portal vein tumor thrombosis and/or extrahepatic metastasis, who visited the Department of Hepatology, Kyoundo Hospital, Tokyo, Japan, between December 2008 and September 2011, were also enrolled (n = 20). This study was carried out in accordance with the ethical guidelines of the 1975 Declaration of Helsinki and was approved by the Institutional Research Ethics Committees of the authors' institutions. Informed consent was obtained for the use of the samples in this study.

Measurement of MtCK activity

The MB fraction of creatine kinase (CK-MB), known as a serum marker for myocardial infarction, has been conventionally measured using an immuno-inhibition method against the MM fraction of creatine kinase (CK-M); however, the appearance of MtCK in serum can render this measurement inaccurate. To resolve this problem, a novel immuno-inhibition method has been recently developed using two types of anti-MtCK monoclonal antibodies in addition to an anti-CK-M antibody [19]. Using this new method, we were able to focus on the measurement of MtCK activity, adjusting the results according to the presence or absence of anti-MtCK monoclonal antibodies during CK-MB measurement. To measure ubiquitous and sarcomeric MtCK, anti-ubiquitous MtCK antibody and anti-sarcomeric MtCK antibody (a kind gift from Shino-test Corporation and Sysmex Corporation) [19] were used, respectively. JCA-BM8040 (JEOL, Tokyo, Japan) was used as an automatic analyzer.

The regression line of this assay was linear up to at least 1800 U/L. The minimum detection limit was 1.9 U/L. The within-run coefficient variations were 3.1% and 0.8% at the mean MtCK activities of 25.7 and 64.4 U/L, respectively. The between-run coefficient variations were 2.3% for both the mean MtCK activities of 24.0 and 59.5 U/L.

Radiofrequency ablation (RFA)

Among 147 patients with HCC, 112 patients were treated using RFA with curative intent, the detailed procedure of which has been meticulously described elsewhere [22]. In some of these patients, serum MtCK activity was measured after RFA.

MtCK and other CK isoenzyme analyses using electrophoresis and immunoblotting

MtCK and other CK isoenzyme analyses were performed using electrophoresis according to a previously described method [19], where 30 μl of serum was analyzed with or without prior incubation with 1 μl of anti-CK-M antibody (a kind gift from Shino-test Corporation and Sysmex Corporation) for 5 min at room temperature.

The serum samples were also applied to sodium dodecyl sulfate polyacrylamide gel electrophoresis under reducing conditions, and then transferred to a polyvinylidene difluoride membrane (Invitrogen, Carlsbad, CA, USA). After blocking the membrane with the agent derived from skim milk (Block Ace; Dainippon Sumitomo Pharmaceutical Co., Ltd., Osaka, Japan), it was incubated with anti-ubiquitous MtCK antibody (dilution, 1:1000) or anti-CK-B antibody (dilution, 1:1000, Sigma–Aldrich, Inc., St. Louis, MO USA) overnight at 4 °C and then with horseradish peroxidase-conjugated secondary antibody (dilution, 1:1000) for 1 h at room temperature. Immunoreactive proteins were visualized using a chemiluminescence kit (GE Healthcare, Little Chalfont, Buckinghamshire, UK), and recorded using a LAS-4000 image analyzer (Fuji Film, Tokyo, Japan).

Quantitative real-time PCR

Total RNA of human HCC cell lines, JHH7, Alex, HuH7, and HepG2 (obtained from Health Science Research Resources Bank, Japan Health Science Foundation) was extracted using TRIZOL reagent (Invitrogen). Human liver RNA was purchased from Cell Applications Inc. (San Diego, CA, USA). One microgram of purified total RNA was transcribed using a SuperScriptTM First-Strand Synthesis System for RT-PCR (Invitrogen). A real-time PCR was performed with the same sets of ubiquitous *MtCK* primers (5′-*CCTGCTAAGCAAAGATAGCC*-3′ and 5′-*TAATGCTTGGTGTGGAT*GAC-3′) and *18s* rRNA primers (5′-GTAACCCGTTGAACCCCATT-3′ and 5′-CCATCCAATCGGTAGTAGCG-3′). The PCR reactions were performed in a Light Cycler 2.0 instrument (Roche Molecular Diagnostics, Mannheim, Germany) using the LightCycler FastStart DNA Master SYBR Green I kit (Roche Molecular Diagnostics). The samples were incubated initially for 10 min at 95 °C, followed by 45 cycles of 95 °C for 10 sec, 60 °C for 10 sec, and 72 °C for 10 sec. The relative amount of ubiquitous *MtCK* was determined from the respective standard curves and normalized to the signal of *18s* rRNA.

Statistical analysis

Comparisons of the distributions of demographic and clinical variables among the groups were performed using Mann–Whitney U test or Chi-square test. Wilcoxon's signed rank test was used to compare the serum MtCK activities before and after RFA. A two-sided significance level of 5% was used for all the analyses. Data processing and analysis were performed using SPSS software version 17.0 or 19.0 (SPSS, Inc., Chicago, IL).

Results

Subjects

Clinical and laboratory variables of the cirrhotic patients with or without HCC are shown in Table 1. These variables did not differ

Table 1. Characteristics of cirrhotic patients with and without HCC.

	Cirrhotic patients		*p* value
	without HCC	with HCC	
No. of patients	92	147	
Age (yr)	67.9 ± 10.8	71.0 ± 7.2	0.127
Gender (M:F)	34:58	92:55	<0.001
HBV:HCV	5:87	12:135	0.425
AST (IU/L)	55.1 ± 30.5	60.9 ± 37.2	0.319
ALT (IU/L)	46.3 ± 31.5	47.0 ± 32.2	0.900
Albumin (g/dl)	3.7 ± 0.6	3.5 ± 0.6	0.001
Bilirubin (mg/dl)	1.2 ± 1.1	1.1 ± 0.7	0.332
MtCK (U/L)	7.4 ± 6.2	14.3 ± 11.9	<0.001
AFP (ng/ml)	20.5 ± 38.5	289.6 ± 1066.3	<0.001
DCP (mAU/ml)	19.1 ± 12.3	318.7 ± 1065.2	<0.001
Platelet count (×10^4/μl)	9.5 ± 4.4	9.6 ± 4.2	0.887
APRI	13.9 ± 10.6	14.1 ± 10.1	0.450
Number of lesions	n.a.	2.8 ± 3.1	
1		73	
2		25	
3		18	
4		9	
≥5		22	
Maximum tumor diameter (cm)	n.a.	1.9 ± 1.1	
≤2.0		107	
2.1-3.0		26	
>3.0		14	
Portal vein thrombosis	n.a.	7	
Metastasis	n.a.	0	

Data provided are means ± SD.
n.a., not available.

significantly between the two groups, except for sex, serum albumin level, serum MtCK activity, serum AFP level and serum DCP level. Serum MtCK activity did not differ between men and women in either the healthy subjects (3.2 ± 1.1 and 3.6 ± 1.4 U/L, respectively; $p = 0.535$) or the subjects overall (10.4 ± 10.9 and 9.4 ± 8.8 U/L, respectively; $p = 0.623$). A significant but small difference was seen in serum albumin levels between cirrhotic patients with HCC and those without HCC; however, other variables suggesting the grade of liver fibrosis, such as serum bilirubin level, platelet count, or the aspartate aminotransferase-to-platelet ratio index (APRI; calculated as aspartate aminotransferase [U/L]/upper normal × 100/platelet count [10^9/L]) were not significantly different between the two groups (Table 1).

Increased serum MtCK activity in patients with HCC

Serum MtCK activity was significantly elevated in cirrhotic patients with HCC, compared with healthy subjects, as shown in Fig. 1 (p <0.001): the mean serum MtCK activity was 14.3 U/L in the former group and 3.4 U/L in the latter group. Serum MtCK activity in the cirrhotic patients without HCC was 7.4 U/L, which

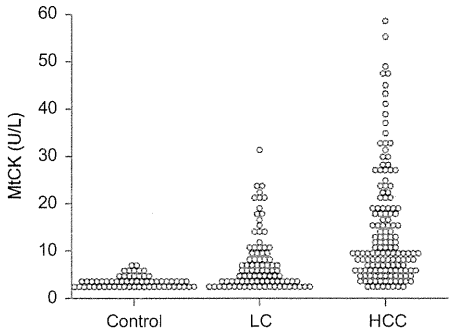

Fig. 1. Scatter plots showing serum MtCK activity in control subjects (Control), cirrhotic patients without HCC (Cirrhosis), and cirrhotic patients with HCC (HCC). Mean serum MtCK activity in cirrhotic patients with HCC (14.3 U/L) was significantly higher than that in patients without HCC (7.3 U/L; p <0.001) and control subjects (3.4 U/L; p <0.001).

was also significantly higher than that in the healthy subjects (p <0.001). However, serum MtCK activity was significantly higher in the cirrhotic patients with HCC than in those without HCC, as depicted in Fig. 1 (p <0.001). In addition, serum MtCK activity did not differ between patients with HBV and those with HCV (14.3 ± 11.1 and 11.3 ± 10.5 U/L, respectively; $p = 0.163$). Serum MtCK activity in the HCC patients according to BCLC stage is shown in Table 2, in which the significant correlation between serum MtCK activity and BCLC stage was not observed. Serum MtCK activity in patients with a single HCC ⩽2 cm was increased and not different from that in patients with HCC with multiple lesions and/or larger than 2 cm (Table 2).

Because consecutive HCC patients with cirrhosis, who visited our department between January and April 2010, were enrolled in this study, there were 12 patients, who developed HCC for the first time, while recurrences had occurred in 135 patients. Serum MtCK activity was not significantly different between the two groups; 10.0 ± 5.2 U/L in the former, and 14.7 ± 12.2 U/L in the latter ($p = 0.430$).

We could measure serum MtCK activity in 14 patients, who had higher levels of serum MtCK activity prior to the treatment and underwent RFA with curative intent, at 2 to 12 weeks following the treatment. In these patients, although its number was small, serum MtCK activity was decreased significantly after RFA (n = 14, $p = 0.001$).

Sensitivity and specificity of MtCK, AFP, and DCP for differentiating HCC from cirrhosis without HCC

To examine a potential predictability of serum MtCK activity for HCC, receiver operating curves (ROCs) were plotted to define the optimal cut-off values and to identify the sensitivity and specificity of MtCK, AFP, and DCP for differentiating cirrhotic patients with HCC from those without HCC (Fig. 2 and Table 3). The area under the receiver operating curve (AUROC) for serum MtCK activity was 0.722 (95%CI: 0.658 – 0.786), with a sensitivity of 62.6%, a specificity of 70.7%, a positive predictive value of 77.3%, a negative predictive value of 54.2%, and a cut-off point of 8.0 U/L; the AUROC for serum AFP level was 0.713 (95%CI: 0.649 – 0.777), with a sensitivity of 52.4%, a specificity of 76.8%, and a cut-off of 20 ng/ml (recommended cut-off for AFP); and the AUROC for serum DCP level was 0.764 (95%CI: 0.705 –

Table 2. HCC stage and serum MtCK activity.

	With the 1st occurrence *vs.* recurrence[b]	
	Number of patients	MtCK (U/L)
BCLC[a] stage		
0	3 *vs.* 32	14.6 ± 4.6[c] *vs.* 9.9 ± 8.3
A	3 *vs.* 53	8.5 ± 3.0 *vs.* 15.3 ± 12.6
B	6 *vs.* 27	8.5 ± 5.4 *vs.* 16.3 ± 14.2
C	0 *vs.* 7	n.a.[d] *vs.* 13.9 ± 16.1
D	0 *vs.* 16	n.a. *vs.* 19.7 ± 10.1
Single lesion ≤2 cm	59	14.2 ± 10.9
Others	88	14.4 ± 12.5

[a]Barcelona Clinic Liver Cancer.
[b]BCLC stage at the first diagnosis of patients with recurrence was BCLC 0, 54; A, 58; B, 28; C, 5; D, 1; unknown, 1. Treatment at the first diagnosis of all patients was surgery, 19; RFA, 76; percutaneous ethanol injection therapy, 8; percutaneous microwave coagulation therapy, 1; transcatheter arterial chemoembolization, 42; unknown, 1.
[c]Data provided are means ± SD.
[d]Not applicable.

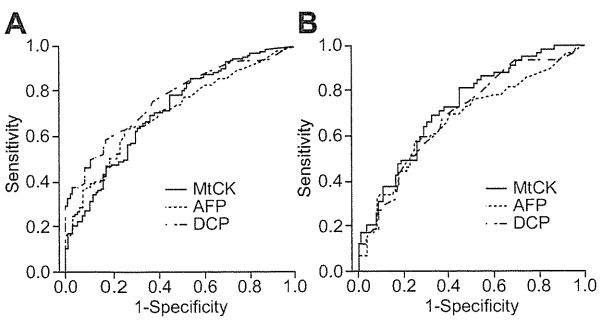

Fig. 2. ROC curves comparing MtCK, AFP, and DCP in patients with cirrhosis without HCC and with HCC. The ROC statistical analyses were performed to compare the diagnostic accuracy of MtCK, AFP, and DCP for (A) HCC in cirrhotic patients and for (B) HCC of a single lesion and smaller than 2 cm.

0.822), with a sensitivity of 40.1%, a specificity of 91.9%, and a cut-off of 40 mAu/ml (recommended cut-off for DCP; Fig. 2). Thus, MtCK had an AUROC between that of AFP and DCP.

Using a cut-off value of 8.0 U/L, serum MtCK activity was elevated in 37 of 70 HCC patients with an AFP <20 ng/ml, in 55 of 87 HCC patients with a DCP <40 mAu/ml, and in 21 of 44 patients with an AFP <20 ng/ml and a DCP <40 mAu/ml (Fig. 3). When AFP and MtCK were combined for the diagnosis of HCC, the sensitivity was increased to 77.6%; when DCP and MtCK were combined, the sensitivity was increased to 78.2%. On the other hand, 23 HCC patients (16%) were not diagnosed even with MtCK, AFP, and DCP, in which serum MtCK activity was 4.7 ± 1.8 U/L and HCC had a maximum diameter of 1.7 ± 0.9 cm with 1.8 ± 1.8 lesions.

Because ultrasonography plays an important role in HCC surveillance in Japan, especially in patients with cirrhosis, we wondered whether MtCK could support the diagnostic capability of ultrasonography. In this study, ultrasonography was not capable of detecting HCC in 13 of 147 HCC patients. Among these patients, serum MtCK activity was higher than the cut-off value

Table 3. The area under the receiver operating curve (AUROC) for MtCK, AFP, and DCP predicting HCC predominantly with recurrence.

Parameters	AUROC (95% CI)
All HCC	
MtCK	0.722 (0.658-0.786)
AFP	0.713 (0.649-0.777)
DCP	0.764 (0.705-0.822)
HCC with a single lesion ≤2 cm	
MtCK	0.729 (0.648-0.809)
AFP	0.672 (0.581-0.762)
DCP	0.694 (0.608-0.780)

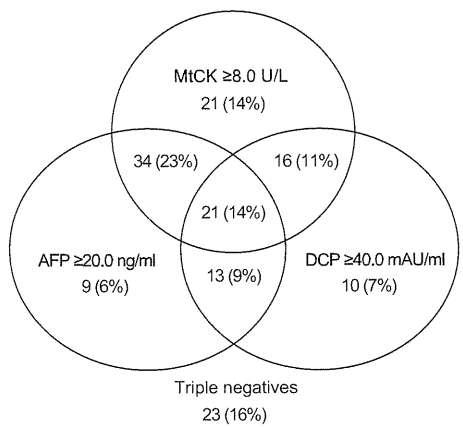

Fig. 3. Number of HCC patients with positive or negative MtCK, AFP, and DCP. The cut-off for serum MtCK activity for the prediction of HCC was defined as 8.0 U/L. The cut-offs for AFP and DCP for the prediction of HCC were 20 ng/ml and 40 mAu/ml, respectively.

of 8.0 U/L in 7 patients (53.8%), among whom only MtCK, but not AFP or DCP levels, were higher than the cut-off values in three patients (23.1%). These results suggest that MtCK activity may support ultrasonography findings for the diagnosis of HCC. In the population of ultrasound-detected HCC, HCC was predictable in 84.7% of those patients with combination of MtCK with a cut-off of 5.6 U/L and AFP with a cut-off of 20 ng/ml, and in 88.3% with combination of MtCK, AFP, and DCP with a cut-off of 40 mAu/ml. On the other hand, in the population of ultrasound-undetected HCC, HCC was predictable in 76.9% of those patients with combination of MtCK with a cut-off of 5.4 U/L and AFP with a cut-off of 20 ng/ml, and in 84.6% with combination of MtCK, AFP, and DCP with a cut-off of 40 mAu/ml.

In addition, serum MtCK activity was higher than 8.0 U/L in 66.7% patients with first HCC occurrence and in 62.2% patients with HCC recurrence. When analyzed among patients with a maximum HCC diameter ⩽2 cm with single nodule, the AUROC for MtCK was higher than AFP or DCP (Fig. 2 and Table 3), and serum MtCK activity was higher than 8.0 U/L in 64.4% of those patients, whereas in 62.6% of whole patients. On the other hand, because patients in the current original cohort had mostly small